

Author Query Form

Journal code: AOS

Transmittal No.: AOS1923

Dear Author,

During the preparation of your manuscript for typesetting, some questions have arisen. They are listed below. Please check your proof carefully and mark all corrections at the appropriate place in the proof (e.g., by using on-screen annotation in the PDF file) or compile them in a separate list. Note: if you opt to annotate the file with software other than Adobe Reader then please also highlight the appropriate place in the PDF file.

Any queries or remarks that have arisen during the processing of your manuscript are listed below and highlighted by flags in the proof.

| Location in article | Query / Remark: Click on the Q link to find the query's location in text Please insert your reply or correction at the corresponding line in the proof |
|------------------------|--|
| | <p>Please take a moment to read through the instructions in the email and submit the linked forms. We MUST have the signed copyright transfer (from all authors) before your article can be published.</p> <p>The bibliography of your paper was retrieved from MathSciNet applying an automated procedure. Please compare original reference list with references retrieved from MathSciNet and indicate those entries which lead to mistaken sources in automatically generated Reference list.</p> <p>Please note that according to a change in journal style only the division, organization and e-mail address will appear in the address on the first page. Additional information can be included in the Acknowledgments section if necessary.</p> |

1
 2 **ASYMPTOTIC RISK AND PHASE TRANSITION OF l_1 -PENALIZED ROBUST**
 3 **ESTIMATOR**
 4

5 BY HANWEN HUANG¹
 6

7 ¹*Department of Epidemiology and Biostatistics, University of Georgia, huanghw@uga.edu*
 8

9 Mean square error (MSE) of the estimator can be used to evaluate the
 10 performance of a regression model. In this paper, we derive the asymptotic
 11 MSE of l_1 -penalized robust estimators in the limit of both sample size n and
 12 dimension p going to infinity with fixed ratio $n/p \rightarrow \delta$. We focus on the l_1 -
 13 penalized least absolute deviation and l_1 -penalized Huber's regressions. Our
 14 analytic study shows the appearance of a sharp phase transition in the two-
 15 dimensional sparsity-undersampling phase space. We derive the explicit
 16 formula of the phase boundary. Remarkably, the phase boundary is identical to
 17 the phase transition curve of LASSO which is also identical to the previously
 18 known Donoho–Tanner phase transition for sparse recovery. Our derivation
 19 is based on the asymptotic analysis of the generalized approximation passing
 20 (GAMP) algorithm. We establish the asymptotic MSE of the l_1 -penalized
 21 robust estimator by connecting it to the asymptotic MSE of the correspond-
 22 ing GAMP estimator. Our results provide some theoretical insight into the
 23 high-dimensional regression methods. Extensive computational experiments
 24 have been conducted to validate the correctness of our analytic results. We
 25 obtain fairly good agreement between theoretical prediction and numerical
 26 simulations on finite-size systems.
 27

28 **1. Introduction.**
 29

30 **1.1. Motivation.** Consider the problem of reconstructing $\beta_0 \in \mathbb{R}^p$ from the measure-
 31 ments
 32

33 (1.1)
$$\mathbf{y} = \mathbf{X}\beta_0 + \boldsymbol{\varepsilon},$$

 34

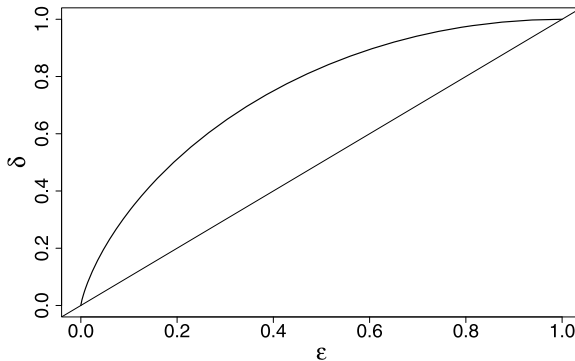
35 where $\mathbf{X} \in \mathbb{R}^{n \times p}$ is the design matrix and $\boldsymbol{\varepsilon}$ denotes random noise which has zero-mean com-
 36 ponents $\boldsymbol{\varepsilon} = (\varepsilon_1, \dots, \varepsilon_n)^T$ i.i.d. with distribution p_ε . The l_1 -penalized least square regression,
 37 also called LASSO [29], is one of the successful methods for estimating β_0 . The performance
 38 of LASSO has been studied in the literature by evaluating the upper bound of its mean square
 39 error (MSE). For instance, [11] prove that the MSE of LASSO estimator is bounded by the
 40 size of the error multiplying by a constant. These types of results are very robust but suffer
 41 from loose constants and cannot provide quantitative recommendations in practice.
 42

43 Inspired by the seminal work of [16], researchers have started performing asymptotic anal-
 44 yses of LASSO under the setting $n, p \rightarrow \infty$ with fixed ratio $n/p \rightarrow \delta$. These type of analyses
 45 can provide sharp quantitative guidelines because they allow to derive exact high-dimensional
 46 limit for the LASSO risk [4]. One interesting result in this direction is the phase transition of
 47 the LASSO minimax risk which is defined as the minimum of the worst-case MSE of LASSO
 48 estimator over the regularization parameter. Let $k = \|\beta_0\|_0$ denote the number of nonzero el-
 49 ements of β_0 and $\epsilon = k/p$ denote the sparsity rate. It was shown in [17] that the LASSO
 50 minimax risk exhibits a phase transition in the two-dimensional phase space $(\delta, \epsilon) \in [0, 1]^2$.
 51 More specifically, a curve $\delta = \delta_c(\epsilon)$ was explicitly computed to divide the phase space into

48 Received December 2018; revised October 2019.
 49

50 **MSC2010 subject classifications.** Primary 62J05, 62J07; secondary 62H12.
 51

52 **Key words and phrases.** Mean square error, minimax, penalized, phase transition, robust.
 53



12 FIG. 1. *LASSO minimax risk phase transition in the plane (ϵ, δ) .* The solid curve represents the phase transition
 13 boundary $\delta = \delta_c(\epsilon)$.

14
 15 two components as shown in Figure 1. The LASSO minimax risk is bounded in the region
 16 $\delta > \delta_c(\epsilon)$ and unbounded in the region $\delta < \delta_c(\epsilon)$. Remarkably, the phase boundary $\delta = \delta_c(\epsilon)$
 17 is identical to the previously known phase transition curve in the problem of reconstructing
 18 the underdetermined linear systems in compressed sensing in the k -sparse noiseless case [13].

19 The least square loss is efficient for normal distributed errors and homogeneous data. How-
 20 ever, data subject to heavy-tailed errors or outliers are commonly encountered in applications.
 21 In this case, the least square estimation is inefficient and can be biased. To overcome this
 22 problem, robust estimators such as those based on the least absolute deviation (LAD) or
 23 Huber-type losses can be useful. Toward this end, penalized robust regression methods have
 24 been proposed in the literature to handle the robustness and sparsity simultaneously. Exam-
 25 ples include [22, 32] among many others. Substantial efforts in this field have been devoted to
 26 developing efficient algorithms for solving the optimization problem and characterizing the
 27 performances of the estimators in low-dimensional setting. However, the characterization of
 28 the penalized robust estimators in the high-dimensional setting has not been explored much.

29 The objective of this paper is to derive the asymptotic MSE of penalized robust estima-
 30 tors. We focus on l_1 -penalized LAD and l_1 -penalized Huber's estimators. Using the results
 31 of asymptotic MSE, we study the phase diagram and associated transitions which describe
 32 the undersampling sparsity trade-off for the reconstruction of signal using penalized robust
 33 estimators. We will show that the phase boundary is identical to the phase transition curve of
 34 LASSO in Figure 1. Our study can provide insight in the theory of regression models.

35 Our analysis is based on the application of the generalized approximate message passing
 36 (GAMP) algorithm to the problem of penalized robust regression. GAMP is a recently de-
 37 veloped iterative algorithm by [24] which is a generalization of the approximate message
 38 passing (AMP) algorithm and can handle not only least square loss but also more general
 39 convex loss functions. The advantage of the GAMP framework is that its asymptotic expres-
 40 sion can be explicitly described by the state evolution equations at each iteration. By showing
 41 that the GAMP estimators converge to the corresponding penalized robust estimators in the
 42 large system limit, we derive the asymptotic MSE of the penalized robust estimator by using
 43 state evolution of the corresponding GAMP estimators. All analytical results are confirmed
 44 by extensive numerical experiments on finite-size systems and our formulas are clarified to
 45 work well even for moderate-size systems.

46
 47 1.2. *Related work.* This phase-transition curve shown in Figure 1 was originally derived
 48 in [13] by methods in combinatorial geometry. Donoho et al. [16] rederived this boundary by
 49 applying the AMP algorithm to the LASSO problem in the noiseless case. General analysis
 50 of phase transition for AMP was presented in [14] for both the noiseless and noisy cases.

1 In the high-dimensional regime of $n, p \rightarrow \infty$ with $n/p = \delta > 1$, [5, 12, 18] examine the
 2 exact stochastic representation for the distribution of non-penalized robust estimators.

3 Bradic [8] proposed a sparse approximate message passing (RAMP) algorithm and ex-
 4 plored the effects of model selection on the estimation of asymptotic MSE for the l_1 -penalized
 5 robust estimators in the setting of both $p < n$ and $p > n$. However, the convergence of the
 6 RAMP estimators to the solution of the penalized robust estimation problem has not been
 7 proved completely. Moreover, they did not investigate the noise sensitivity phase transition
 8 features of the penalized robust estimators. The prediction of phase transitions for different
 9 denoisers besides the soft thresholding one has been studied in [14], but the results are still
 10 based on least square loss.

11

12 2. Asymptotic behavior of l_1 -penalized robust estimator.

13
 14 2.1. *l₁-Penalized robust estimator.* For problem (1.1), we are interested in estimating β_0
 15 using the following l_1 -penalized robust estimators:

16
 17 (2.1)
$$\hat{\beta} = \underset{\beta \in R^p}{\operatorname{argmin}} \left\{ \sum_{i=1}^n \rho(y_i - \mathbf{x}_i^T \beta) + \lambda \sum_{j=1}^p |\beta_j| \right\},$$
 18

19 where $\lambda > 0$ is the tuning parameter for penalty. Here, the loss function $\rho : \mathbb{R} \rightarrow \mathbb{R}_+$ is a
 20 nonnegative convex function. Examples of the loss function include:

21
 22 • Least square loss: $\rho(u) = \frac{1}{2}u^2$.
 23 • Least absolute deviation (LAD) loss: $\rho(u) = |u|$.
 24 • Huber's loss:

25
 26
$$\rho(u) = \begin{cases} \frac{u^2}{2} & |u| \leq \gamma, \\ \gamma|u| - \frac{\gamma^2}{2} & |u| > \gamma, \end{cases}$$
 27
 28
 29

30 where $\gamma > 0$ is a fixed positive constant.

31 The regression model based on least square loss is also called LASSO and has been well
 32 studied. Here, we consider the robust regression model based on LAD loss and Huber's loss.
 33 The robust regression is an alternative to least square regression when the data subject to
 34 heavy-tailed errors or are contaminated with outliers. It can also be used for the purpose of
 35 detecting influential observations. Given a vector $\mathbf{v} \in \mathbb{R}^p$ and a scalar function $f : \mathbb{R} \rightarrow \mathbb{R}$, we
 36 write $f(\mathbf{v})$ for the vector obtained by applying f componentwise. Further, $\langle \mathbf{v} \rangle = p^{-1} \sum_{i=1}^p v_i$
 37 is the average of the vector \mathbf{v} , and \mathbf{X}^T is the transpose of matrix \mathbf{X} .

38
 39 2.2. *Generalized approximate message passing algorithm.* Many algorithms have been
 40 developed in the literature to solve the optimization problem (2.1). Here, we use the gen-
 41 eralized approximate message passing algorithm (GAMP). Our goal is to study the asymptotic
 42 behavior of the regularized robust estimators (2.1) in the limit of $n, p \rightarrow \infty$ with fixed ra-
 43 tio $n/p = \delta$. We start from the asymptotic behavior of the corresponding GAMP estimators
 44 in the large system limit which can be well characterized by a simple set of state evolution
 45 equations. Then we show that the regularized robust estimators asymptotically converge to
 46 the corresponding GAMP estimators.

47 Approximate message passing algorithm (AMP) is a recently developed optimization
 48 method for solving the LASSO minimization problem [16]. The advantage of the AMP
 49 framework is that it provides an exact expression for the asymptotic MSE of the LASSO
 50 estimator instead of an upper bound. AMP has been extended to GAMP in [24] for solving

51

1 general convex optimization problem. In order to apply GAMP to the problem (2.1), we first
 2 need to define the following two functions:

$$(2.2) \quad \eta(a, b) = \operatorname{argmin}_{\beta} \left\{ |\beta| + \frac{1}{2b} (\beta - a)^2 \right\} = (|a| - b)_+ \operatorname{sign}(a),$$

$$(2.3) \quad G_0(a, b) = b \partial \rho(\hat{u}(a, b)),$$

7 where $\partial \rho(\cdot)$ represents the subgradient of $\rho(\cdot)$ function and

$$(2.4) \quad \hat{u}(a, b) = \operatorname{argmin}_u \left\{ \rho(u) + \frac{1}{2b} (u - a)^2 \right\}.$$

11 Based on the definition of $G_0(a, b)$, it can be easily shown that

$$(2.5) \quad G_0(a, b) = a - \hat{u}(a, b).$$

14 For the LAD loss $\rho(u) = |u|$, (2.4) gives

$$\hat{u}(a, b) = \operatorname{sign}(a) (|a| - b)_+,$$

16 which leads to

$$(2.6) \quad G_0(a, b) = \begin{cases} a & |a| \leq b, \\ b & a > b, \\ -b & a < -b. \end{cases}$$

22 For Huber's loss, (2.4) gives

$$\hat{u}(a, b) = \begin{cases} \frac{a}{1+b} & |a| \leq (1+b)\gamma, \\ a - \gamma b & a > (1+b)\gamma, \\ a + \gamma b & a < -(1+b)\gamma \end{cases}$$

27 which leads to

$$(2.7) \quad G_0(a, b) = \begin{cases} \frac{b}{1+b} a & |a| \leq (1+b)\gamma, \\ \gamma b & a > (1+b)\gamma, \\ -\gamma b & a < -(1+b)\gamma. \end{cases}$$

33 Let $\{\theta_t, a_t, \pi_t, \omega_t\}_{t \geq 0}$ denote four sequences of nonnegative parameters. Starting with ini-
 34 tial conditions $\beta^0 = 0 \in \mathbb{R}^p$, $a_0 = 1$ and $G_0(\mathbf{z}^{-1}, a_{-1}) = 0 \in \mathbb{R}^n$, the general form of GAMP
 35 algorithm for (2.1) constructs a sequence of estimates $\beta^t \in \mathbb{R}^p$ and residuals $\mathbf{z}^t \in \mathbb{R}^n$ accord-
 36 ing to the iteration

$$(2.8) \quad \begin{cases} \mathbf{z}^t = \mathbf{y} - \mathbf{X}\beta^t + \frac{1}{\omega_{t-1}} G_0(\mathbf{z}^{t-1}, a_{t-1}) \pi_{t-1}, \\ \beta^{t+1} = \eta \left(\beta^t + \frac{1}{\omega_t} \mathbf{X}^T G_0(\mathbf{z}^t, a_t), \theta_t \right), \end{cases}$$

42 with the parameters $\theta_t, a_t, \pi_t, \omega_t$ updated through

$$(2.9) \quad \begin{cases} \pi_t = \frac{1}{\delta} \left(\partial_1 \eta \left(\beta^{t-1} + \frac{1}{\omega_{t-1}} \mathbf{X}^T G_0(\mathbf{z}^{t-1}, a_{t-1}), \theta_{t-1} \right) \right), \\ a_t = \frac{a_{t-1} \pi_{t-1}}{\omega_{t-1}}, \\ \omega_t = \langle \partial_1 G_0(\mathbf{z}^t, a_t) \rangle, \\ \theta_t = \frac{\lambda a_t}{\omega_t}, \end{cases}$$

1 where ∂_1 represents the derivative over the first argument of the function. A detailed derivation
 2 of (2.8) and (2.9) is provided in the supplementary material [19]. The connection of
 3 (2.8) and (2.9) to the l_1 -penalized robust estimator (2.1) can be formalized by the proposition
 4 below.

5 **PROPOSITION 2.1.** *Let (β^*, \mathbf{z}^*) be a fixed point of the iteration (2.8) for $\theta_t = \theta_*$, $a_t = a_*$,
 6 $\pi_t = \omega_t = \pi_*$ fixed. Then β^* is a minimum of the cost function (2.1) for
 7*

8 (2.10)
$$\lambda = \frac{\theta_* \pi_*}{a_*}.$$
 9
 10

11 As a consequence of this proposition, if the estimates β^t based on (2.8) and (2.9) converge,
 12 then we are guaranteed that the limit is a l_1 -penalized robust estimator.

13 Although GAMP has been successfully applied to many problems, its convergence is still
 14 not fully understood [25, 31]. Various modification procedures have been proposed to im-
 15 prove the convergence of GAMP; see, for example, [26, 28]. To facilitate the convergent
 16 study, here we fix certain parameters throughout the iteration to its fixed-point values. For
 17 this purpose, we take $\omega_t = \pi_*$, the fixed point of π_t , and choose θ_t in a way that will be
 18 discussed in Section 2.4. Let

19 (2.11)
$$G(a, b) = \frac{1}{\pi_*} G_0(a, b)$$
 20
 21

22 denote the rescaled min regularized effective score function, we eventually take the following
 23 form of GAMP algorithm:

24 (2.12)
$$\begin{cases} \mathbf{z}^t = \mathbf{y} - \mathbf{X}\beta^t + \frac{1}{\delta} G(\mathbf{z}^t, a_t) \langle \partial_1 \eta(\beta^t + \mathbf{X}^T G(\mathbf{z}^t, a_t), \theta_t) \rangle, \\ \beta^t = \eta(\beta^{t-1} + \mathbf{X}^T G(\mathbf{z}^{t-1}, a_{t-1}), \theta_{t-1}), \end{cases}$$
 25
 26

27 where the sequence $\{a_t\}_{t \geq 0}$ is determined by

28 (2.13)
$$\langle \partial_1 G(\mathbf{z}^t, a_t) \rangle = 1.$$
 29
 30

31 The RAMP algorithm proposed in [8] chooses $\omega_t = \|\beta_0\|_0/(p\delta)$, where $\|\beta_0\|_0$ denotes the
 32 number of nonzero elements in the true coefficient vector. The advantage of the choice $\omega_t =$
 33 π_* over other choices is that it is more relevant for mathematical analysis. Particularly, as
 34 it will be discussed below, it allows us to establish the convergence of GAMP in a more
 35 convenient way.

36 **2.3. State evolution of GAMP.** It has been shown in [3] that AMP algorithm has several
 37 unique advantages. Particularly, the asymptotic limit of the AMP estimates as $n, p \rightarrow \infty$
 38 for any fixed t can be described by the state evolution (SE). The SE not only predicts the
 39 evolution of numerical statistical properties of β^t with the iteration number t , it also correctly
 40 predicts the success/failure to converge to the correct result.

41 We will show that the GAMP algorithm enjoys the same properties. We will consider
 42 sequences of instances of increasing sizes which are completely determined by the measure-
 43 ment matrix \mathbf{X} , the signal β_0 , and the error vector $\boldsymbol{\varepsilon}$. We assume the following conditions in
 44 order for SE to hold.

45
 46 **ASSUMPTION 1.** $n/p \rightarrow \delta \in (0, \infty).$ 47
 48

49 **ASSUMPTION 2.** The empirical distribution of the entries of β_0 converges weakly to
 50 a probability measure p_{β_0} on \mathbb{R} with bounded second moment. Further $\frac{1}{p} \sum_{i=1}^p \beta_{0,i}^2 \rightarrow$
 $E_{\beta_0}(\beta_0^2).$ 51

1 ASSUMPTION 3. The empirical distribution of the entries of $\boldsymbol{\varepsilon}$ converges weakly to a
 2 probability measure p_ε on \mathbb{R} with bounded second moment. Further $\frac{1}{n} \sum_{i=1}^n \varepsilon_i^2 \rightarrow E_\varepsilon(\varepsilon^2)$.
 3

4 ASSUMPTION 4. The entries of \mathbf{X} are i.i.d. normal with mean 0 and variance $1/n$.
 5

6 Note that the hypothesis of Gaussian measurement matrix \mathbf{X} (Assumption 4) is necessary
 7 for the proof technique to be applicable. Extensive numerical simulations carried out in [17]
 8 showed that, for LASSO, the result is universal over a broader class of i.i.d. matrices. Re-
 9 cently, [6] generalizes the SE result for AMP to standard Gaussian design with nonseparable
 10 denoisers. This work enables the applicability of AMP to Gaussian design with nontrivial
 11 covariance $\boldsymbol{\Sigma}$ and a separable denoiser by a change of variable $\tilde{\mathbf{X}} \rightarrow \boldsymbol{\Sigma}^{-1/2} \mathbf{X}$, $\tilde{\boldsymbol{\beta}}_0 \rightarrow \boldsymbol{\Sigma}^{1/2} \boldsymbol{\beta}_0$.
 12 However, the challenge of this extension is that the convergence of AMP under general non-
 13 i.i.d. matrices has not been fully understood. In fact, recent works in [25, 31] have shown that,
 14 even for the simplest least square loss, GAMP can diverge under mildly ill-conditioned \mathbf{X} .

15 We say a function $\psi : \mathbb{R}^k \rightarrow \mathbb{R}$ is pseudo-Lipschitz if there exists a constant $L > 0$ such
 16 that for all $\mathbf{x}, \mathbf{y} \in \mathbb{R}^k : |\psi(\mathbf{x}) - \psi(\mathbf{y})| \leq L(1 + \|\mathbf{x}\|_2 + \|\mathbf{y}\|_2)\|\mathbf{x} - \mathbf{y}\|_2$. The following propo-
 17 sition is a simple application of the existing results in [8]. It shows that the GAMP iterations
 18 (2.12) and (2.13) admit a high-dimensional limit as $n, p \rightarrow \infty$ with fixed $n/p = \delta$. The proof
 19 is still included in the Appendix for the completeness of the paper.
 20

21 PROPOSITION 2.2. Let $\psi : \mathbb{R} \times \mathbb{R} \rightarrow \mathbb{R}$ be a pseudo-Lipschitz function. Then, under
 22 Assumptions 1–4, almost surely

$$23 \lim_{p \rightarrow \infty} \frac{1}{p} \sum_{i=1}^p \psi(\beta_i^{t+1}, \beta_{0,i}) = E\{\psi(\eta(\beta_0 + \tau_t Z, \theta_t), \beta_0)\},$$

$$26 \lim_{n \rightarrow \infty} \frac{1}{n} \sum_{i=1}^n \psi(z_i^t, \varepsilon_i) = E\{\psi(\varepsilon + \sigma_t Z, \varepsilon)\},$$

29 where $Z \sim N(0, 1)$ is independent of $\beta_0 \sim p_{\beta_0}$ and $\varepsilon \sim p_\varepsilon$. The state evolution sequences
 30 $\{\tau_t^2, \sigma_t^2\}_{t \geq 0}$ are obtained by the following iterative equations:
 31

$$(2.14) \quad \tau_t^2 = E\{G(\varepsilon + \sigma_t Z, a_t)^2\},$$

$$(2.15) \quad \sigma_t^2 = \frac{1}{\delta} E\{(\eta(\beta_0 + \tau_{t-1} Z, \theta_{t-1}) - \beta_0)^2\},$$

35 with the parameters a_t determined by

$$(2.16) \quad E\{\partial_1 G(\varepsilon + \sigma_t Z, a_t)\} = 1.$$

38 According to the standard weak convergence arguments, Proposition 2.2 indicates that
 39 the empirical distribution of the entries of the GAMP estimator $\boldsymbol{\beta}^t$ converges weakly to the
 40 distribution of the random variable $\eta(\beta_0 + \tau_{t-1} Z, \theta_{t-1})$ with $Z \sim N(0, 1)$ independent of β_0 .
 41 Similarly, the empirical distribution of the entries of the residuals \mathbf{z}^t converges weakly to the
 42 distribution of the random variable $\varepsilon + \sigma_t Z$ with $Z \sim N(0, 1)$ independent of ε .
 43

44 2.4. *Fixed-point equations and convergence.* Define $\tau_\star, \sigma_\star, a_\star$ and θ_\star the solutions of the
 45 SE fixed-point equations:
 46

$$(2.17) \quad \tau_\star^2 = E\{G(\varepsilon + \sigma_\star Z, a_\star)^2\},$$

$$(2.18) \quad \sigma_\star^2 = \frac{1}{\delta} E\{(\eta(\beta_0 + \tau_\star Z, \theta_\star) - \beta_0)^2\},$$

$$(2.19) \quad 1 = E\{\partial_1 G(\varepsilon + \sigma_\star Z, a_\star)\}.$$

1 Clearly, the solutions depend on δ as well as the distributions p_{β_0} and p_ε . Then the quantity
 2 π_\star can be obtained as

3

4 (2.20)
$$\pi_\star = \frac{1}{\delta} E\{\partial_1 \eta(\beta_0 + \tau_\star Z, \theta_\star)\}.$$

5

6 Using the explicit forms of (2.6) and (2.7), we obtain the following proposition.

7

8 PROPOSITION 2.3. Define $\tilde{Z} = \varepsilon + \sigma_\star Z$. Then the SE fixed-point equations of l_1 -LAD-
 9 GAMP are

10

11 (2.21)
$$\tau_\star^2 = \frac{1}{\pi_\star^2} [E\{\tilde{Z}^2 I(|\tilde{Z}| \leq a_\star)\} + E\{a_\star^2 I(|\tilde{Z}| \geq a_\star)\}],$$

12

13

14 (2.22)
$$\pi_\star = p(|\tilde{Z}| \leq a_\star) = \frac{1}{\delta} E\{\partial_1 \eta(\beta_0 + \tau_\star Z, \theta_\star)\}.$$

15

16 The SE fixed-point equations of l_1 -Huber-GAMP are

17

18 (2.23)
$$\tau_\star^2 = \frac{1}{\pi_\star^2} \left[E\left\{ \frac{a_\star^2}{(1+a_\star)^2} \tilde{Z}^2 I(|\tilde{Z}| \leq (1+a_\star)\gamma) \right\} \right.$$

19

20
$$\left. + E\{a_\star^2 \gamma^2 I(|\tilde{Z}| \geq (1+a_\star)\gamma)\} \right],$$

21

22

23 (2.24)
$$\pi_\star = \frac{a_\star}{1+a_\star} p(|\tilde{Z}| \leq (1+a_\star)\gamma) = \frac{1}{\delta} E\{\partial_1 \eta(\beta_0 + \tau_\star Z, \theta_\star)\}.$$

24

25 Combining (2.14) and (2.15), we obtain the one-dimensional update for τ_t^2 as

26

27
$$\tau_{t+1}^2 = V(\tau_t^2, \theta_t),$$

28

29 where

30

31 (2.25)
$$V(\tau^2, \theta) = E\{G(\varepsilon + \sigma(\tau, \theta)Z, a(\tau, \theta))^2\},$$

32

33

34 (2.26)
$$\sigma(\tau, \theta)^2 = \frac{1}{\delta} E\{(\eta(\beta_0 + \tau Z; \theta) - \beta_0)^2\}$$

35

36 with $a(\tau, \theta)$ implied by

37

38
$$E\{\partial_1 G(\varepsilon + \sigma(\tau, \theta)Z, a(\tau, \theta))\} = 1.$$

39

40 Now we discuss the choice of the sequence of thresholds θ_t . We take $\theta_t = \alpha \tau_t$ with α
 41 fixed throughout the iterations. As discussed in [4], the main advantage of such choice is that
 42 the convergence of the corresponding recursion $\tau_{t+1}^2 = V(\tau_t^2, \alpha \tau_t)$ can be well established.
 43 Moreover, it is a natural choice from an intuitive point of view. At each step, we apply the
 44 soft thresholding denoiser $\eta(\cdot, \theta_t)$ to an effective observation $\beta_0 + \tau_t Z$ which can be regarded
 45 as the signal β_0 corrupted by Gaussian noise $\tau_t Z$. Therefore, this suggests to choose θ_t pro-
 46 portional to the standard deviation of the noise τ_t . More discussion about the choice of θ_t was
 47 given in [23].

48 Let $\alpha_l = \alpha_l(\delta)$ be the unique nonnegative solution of the equation

49

50 (2.27)
$$2\Phi(-\alpha) = \delta,$$

51

52 where $\Phi(z) = \int_{-\infty}^z \phi(x) dx$ and $\phi(x) = e^{-x^2/2} / \sqrt{2\pi}$ is the standard Gaussian density func-
 53 tion. The following proposition indicates the convergence of the SE equations (2.14) and
 54 (2.15).

1 PROPOSITION 2.4. For any $\sigma^2 > 0$ and $\alpha > \alpha_l$, the fixed-point equation

2 (2.28)
$$\tau^2 = V(\tau^2, \alpha\tau),$$

4 admits at least one solution. Denoting by $\tau_\star^2 = \tau_\star^2(\alpha)$ the largest solution, we have
5 $\lim_{t \rightarrow \infty} \tau_t^2 = \tau_\star^2(\alpha)$ for large enough initial condition $\tau_{t=0}^2$.

7 2.5. *Connection of GAMP to regularized robust estimator.* Before stating our main
8 results, we have to describe a calibration mapping between α and λ which will depend on p_{β_0} .
9 For p_{β_0} , we consider the sparse class

10 (2.29)
$$\mathcal{F}_\epsilon \equiv \{\nu : \nu \text{ is a probability measure with } \nu(\{0\}) \geq 1 - \epsilon\}$$

12 which put mass at least $1 - \epsilon$ on 0. Let $\alpha_u = \alpha_u(\delta)$ be the unique nonnegative solution of the
13 equation

15
$$\epsilon + 2(1 - \epsilon)\Phi(-\alpha) = \delta.$$

17 Clearly, $\alpha_l < \alpha_u$ for $\epsilon > 0$. We then define the function $\alpha \rightarrow \lambda(\alpha)$ on $(0, \infty)$ by

18 (2.30)
$$\lambda(\alpha) = \frac{\alpha\tau_\star(\alpha)\pi_\star(\alpha)}{a_\star(\alpha)}.$$

21 This function defines a correspondence between the threshold $\alpha\tau_\star$ and the regularization
22 parameter λ . We need to invert this function and define $\alpha : (0, \infty) \rightarrow (0, \infty)$ in such a way
23 that

24 (2.31)
$$\alpha(\lambda) = \{a \in (0, \infty) : \lambda(a) = \lambda\}.$$

26 The next result implies that the set on the right-hand side is nonempty and therefore the
27 function $\lambda \rightarrow \alpha(\lambda)$ is well-defined.

29 PROPOSITION 2.5. For any $\sigma^2 > 0$, there exist an $\alpha_{\min} \in [\alpha_l, \alpha_u]$ which depends on p_{β_0}
30 such for any $\alpha > \alpha_{\min}$, the function $\alpha \rightarrow \lambda(\alpha)$ is continuous on the interval (α_{\min}, ∞) with
31 $\lambda(\alpha_{\min}+) = 0$ and $\lim_{\alpha \rightarrow \infty} \lambda(\alpha) = \infty$. Therefore, the function $\lambda \rightarrow \alpha(\lambda)$ satisfying (2.31)
32 exists.

34 State evolution provides the limit of GAMP estimation in the high-dimensional setting.
35 By showing that the GAMP estimator converges to the regularized robust estimator, one can
36 obtain the distributional limit for the latter as well. The following theorem shows that the
37 empirical distribution of the entries of the regularized robust estimator $\hat{\beta}$ from (2.1) con-
38 verges weakly to the distribution of the random variable $\eta(\beta_0 + \tau_\star Z; \theta_\star)$ with $Z \sim N(0, 1)$
39 independent of β_0 .

41 THEOREM 2.1. Under Assumptions 1–4, denote by $f(x)$ the density function for the
42 distribution of error term ε . Further assume that for any $\omega > 0$, there exists a large enough
43 $C > 0$ such that $f(x) > 0$ for all $x \in [-C, C]$ and the probability $p(x \in [-C, C]) \geq 1 - \omega$.
44 Let $\psi : \mathbb{R} \times \mathbb{R} \rightarrow \mathbb{R}$ be a pseudo-Lipschitz function. Then, almost surely

46
$$\lim_{p \rightarrow \infty} \frac{1}{p} \sum_{i=1}^p \psi(\hat{\beta}(\lambda)_i, \beta_{0,i}) = E\{\psi(\eta(\beta_0 + \tau_\star Z, \alpha(\lambda)\tau_\star), \beta_0)\},$$

49 where $Z \sim N(0, 1)$ is independent of $\beta_0 \sim p_{\beta_0}$, $\tau_\star = \tau_\star(\alpha(\lambda))$ is the solution of the fixed-point
50 equation (2.28) with $\alpha = \alpha(\lambda)$.

1 Theorem 2.1 allows us to theoretically study the MSE of the regularized robust estimator.
 2 Using function $\psi(a, b) = (a - b)^2$, we obtain

$$3 \quad 4 \quad 5 \quad \lim_{p \rightarrow \infty} \frac{1}{p} \|\hat{\beta}(\lambda) - \beta_0\|^2 = E\{[\eta(\beta_0 + \tau_\star Z, \alpha(\lambda)\tau_\star) - \beta_0]^2\},$$

6 which depends on $\delta, \lambda, p_{\beta_0}$ and p_ε . Therefore, the asymptotic risk of the regularized robust
 7 estimator can be determined for any specific distributions p_{β_0} and p_ε by solving the fixed-
 8 point equation (2.28). Note that Theorem 2.1 allows us to predict MSE for any fixed λ . This is
 9 different from the traditional large n fixed p situations where the usual value for λ is chosen
 10 growing to 0. We prove Theorem 2.1 by proving the following result.

11

12 THEOREM 2.2. *Under the same assumptions used for Theorem 2.1, we have*

$$13 \quad 14 \quad 15 \quad \lim_{t \rightarrow \infty} \lim_{p \rightarrow \infty} \frac{1}{p} \|\beta^t - \hat{\beta}\|_2^2 = 0,$$

16 almost surely.

17 After establishing the convergence of the state evolution, the proof technique of Theorem 2.2 is very similar to the existing proof techniques used in LASSO paper [4]. For completeness, we outline the main proof in the Appendix and move the technical lemmas into the supplementary material.

22

23 **3. Phase transition and minimax risk.** In this section, we study the minimax risk and
 24 phase transition properties of the l_1 -penalized robust estimator based on the asymptotic re-
 25 sults derived in Section 2. Here, the minimax risk refers to minimizing the worst-case MSE
 26 over λ for estimators based on a specific l_1 -penalized robust method. It is not a minimax over
 27 all possible estimators. We start from the fixed-point equations (2.17)–(2.20) and focus on
 28 two special robust regression methods: l_1 -LAD and l_1 -Huber's regression. The results de-
 29 pend on distributions p_ε and p_{β_0} . We consider the sparse class \mathcal{F}_ϵ defined in (2.29) for p_{β_0}
 30 and have a phase space $0 \leq \epsilon, \delta \leq 1$ expressing different combinations of under-sampling δ
 31 and sparsity ϵ .

32

33 **3.1. Noiseless l_1 -LAD.** Let us first consider the noiseless case, that is, $\sigma_0^2 = 0$. We study
 34 under which condition the original signal β_0 can be correctly reconstructed from the mea-
 35 surement \mathbf{y} using l_1 -LAD regression after appropriately tuning the λ .

36 It is well known that in the problem of reconstructing the underdetermined linear system,
 37 exact reconstruction takes place subject to a trade-off between under-sampling δ and sparsity
 38 ϵ [13]. There is a function $\delta_c(\epsilon)$ whose graph partitions the domain $(\epsilon, \delta) \in [0, 1]^2$ into two
 39 regions, a “success” region, where exact reconstruction occurs, and a “failure” region where
 40 exact reconstruction fails. In the lower region, where $\delta < \delta_c(\epsilon)$, the probability of exact re-
 41 construction tends to zero as $k, n, p \rightarrow \infty$ with $k/p \rightarrow \epsilon$ and $n/p \rightarrow \delta$. In the upper region,
 42 where $\delta > \delta_c(\epsilon)$, the corresponding probability of exact reconstruction tends to one. Hence
 43 the curve $\delta = \delta_c(\epsilon)$ for $0 < \delta < 1$ indicates the precise trade-off between under-sampling and
 44 sparsity.

45 Note that, for LASSO, $\delta_c(\epsilon)$ is independent of the actual signal distribution p_{β_0} . This is
 46 different from the l_p -penalized regressions with $0 \leq p < 1$ studied in [34] in which p_{β_0} has a
 47 substantial effect on the phase transition curve. As shown in [16], the curve $\delta_c(\epsilon)$ admits the
 48 following simple form:

$$49 \quad 50 \quad (3.1) \quad \delta_c(\epsilon) = \frac{2\phi(\alpha_c)}{\alpha_c + 2(\phi(\alpha_c) - \alpha_c\Phi(-\alpha_c))},$$

51

1 where α_c is determined by

$$2 \quad (3.2) \quad \epsilon = \frac{2(\phi(\alpha_c) - \alpha_c \Phi(-\alpha_c))}{\alpha_c + 2(\phi(\alpha_c) - \alpha_c \Phi(-\alpha_c))},$$

3 where $\alpha_c \in [0, \infty)$ is the parameter.

4 The following theorem shows that a phase transition also occurs in the l_1 -LAD regression
5 for noiseless case. The domain has two phases: a “success” phase, where the l_1 -LAD regres-
6 sion succeeds to recover β_0 , and a “failure” phase where it fails to reconstruct β_0 . Moreover,
7 this phase transition boundary is exactly $\delta = \delta_c(\epsilon)$.

8 THEOREM 3.1. *Under Assumptions 1, 2 and 4, denote $\hat{\beta}$ the estimator from (2.1) based
9 on the LAD loss in the noiseless case. For any $\delta > \delta_c(\epsilon)$, we can tune the parameter λ and
10 have $\lim_{p \rightarrow \infty} \frac{1}{p} \|\hat{\beta} - \beta_0\|^2 = 0$ almost surely. Thus we can make consistent estimation for
11 the original signal β_0 in this region. For any $\delta < \delta_c(\epsilon)$, we have $\lim_{p \rightarrow \infty} \frac{1}{p} \|\hat{\beta} - \beta_0\|^2 > 0$
12 almost surely for any tuning parameter λ . Thus the consistent estimation in this region fails.*

13 Theorem 3.1 shows that, in the “success” region, we can tune α such that the equation
14 (2.28) admits a unique solution $\tau_\star = 0$ which corresponds to $\lambda = 0$ for the original problem
15 (2.1) according to the calibration mapping (2.30).

16 3.2. *Noisy l_1 -LAD.* Next, we study the MSE of $\hat{\beta}$ in the noisy case, that is, $\sigma_0^2 \neq 0$. In
17 this case, the probability of exact reconstruction tends to zero and the MSE result depends on
18 p_{β_0} . In the more realistic situation, we do not know p_{β_0} . However, if we consider the sparsity
19 class \mathcal{F}_ϵ and take the worst case MSE over this class and then minimize over λ , we get a
20 result that is independent of p_{β_0} . Toward this end, we define the minimax risk as

$$21 \quad (3.3) \quad M(\delta, \epsilon) = \min_{\lambda} \sup_{p_{\beta_0} \in \mathcal{F}_\epsilon} \lim_{p \rightarrow \infty} \frac{1}{p} \sum_{i=1}^p \{|\hat{\beta}_i(\lambda) - \beta_{0,i}|^2\}.$$

22 That is, the regularization parameter λ is optimally chosen such that the maximal MSE based
23 on a specific l_1 -penalized robust method for the class \mathcal{F}_ϵ is minimized.

24 The following theorem shows that in the presence of noise, the phase space $0 \leq \delta, \epsilon \leq 1$ is
25 partitioned by the curve $\delta = \delta_c(\epsilon)$ into two regions. The minimax risk of l_1 -LAD is bounded
26 throughout the “success” region and unbounded throughout the “failure” region.

27 THEOREM 3.2. *Under Assumptions 1–4 with the condition of bounded second moment
28 for p_{β_0} in Assumption 2 removed, recall that $M(\delta, \epsilon)$ defined in (3.3) denotes the minimax
29 risk of l_1 -LAD. Then, for any $\delta > \delta_c(\epsilon)$, $M(\delta, \epsilon)$ is bounded; for any $\delta < \delta_c(\epsilon)$, $M(\delta, \epsilon)$ is
30 unbounded.*

31 Note that the optimal choice of regularization parameter for minimizing the maximum
32 risk is related to α_c provided by (3.1). The upper bounds for the minimax risk of the sparse
33 regression estimators for (1.1) have been studied in the literature; see, for example, [7, 9, 27,
34 30]. There is a lower bound result in [30] which shows that the lower bound of estimating
35 β in high dimension is $C_1 \frac{\epsilon}{\delta} \{1 + \log(1/\epsilon)\}$ for $1 \leq k \leq (n-1)/4$ and $\Sigma = \mathbf{I}$ (see (6.7) in
36 Proposition 6.4 in [30]). Our results complement this type of “rough and robust” bounds by
37 providing asymptotic formal expression for the MSE of $\hat{\beta}$.

38 Based on Theorem 3.2, in the upper region $\delta > \delta_c(\epsilon)$, we can estimate the actual minimax
39 risk of l_1 -LAD. Denote

$$40 \quad (3.4) \quad M^\star(\epsilon) = \delta_c(\epsilon)$$

1 which is defined in (3.1). It was shown in [17] that the LASSO minimax risk is simply given
 2 by

$$3 \quad (3.5) \quad M(\delta, \epsilon) = \frac{\sigma_0^2 M^*(\epsilon)}{1 - M^*(\epsilon)/\delta} \quad 4 \quad 5$$

6 which does not depend on the distribution p_ϵ . In contrast, the explicit form of minimax risk
 7 of l_1 -LAD depends on the distribution p_ϵ . We consider three different distributions here.
 8

9 **PROPOSITION 3.1.** *Normal random error. Assume that the noise term ϵ follows a normal
 10 distribution $\epsilon \sim N(0, \sigma_0^2)$. Then for $\delta > \delta_c(\epsilon)$, the minimax MSE of l_1 -LAD is*

$$11 \quad (3.6) \quad M(\delta, \epsilon) = \frac{\sigma_0^2 F(c) M^*(\epsilon)}{1 - F(c) M^*(\epsilon)/\delta}, \quad 12 \quad 13$$

14 where

$$15 \quad (3.7) \quad F(c) = \frac{2\Phi(c) - 1 + 2c(c\Phi(-c) - \phi(c))}{(2\Phi(c) - 1)^2}, \quad 16 \quad 17$$

18 where c depends on (ϵ, δ) through $2\Phi(c) - 1 = \frac{M^*(\epsilon)}{\delta}$.
 19

20 Clearly, l_1 -LAD risk (3.6) is larger than the corresponding LASSO risk (3.5) because
 21 $F(c) \geq 1$. It is interesting to check that

$$22 \quad F(c) M^*(\epsilon)/\delta \leq 1. \quad 23$$

24 To show this, notice that $\frac{M^*(\epsilon)}{\delta} = 2\Phi(c) - 1$ which leads to

$$25 \quad (3.8) \quad F(c) M^*(\epsilon)/\delta = \frac{2\Phi(c) - 1 + 2c(c\Phi(-c) - \phi(c))}{2\Phi(c) - 1} \leq 1 \quad 26 \quad 27$$

28 because $c\Phi(-c) \leq \phi(c)$ for any $c \geq 0$. Therefore, for normal distributed ϵ , l_1 -LAD mini-
 29 max risk is larger than LASSO minimax risk. This is consistent with the classical statistical
 30 analysis, that is, least square loss is optimal for Gaussian errors.
 31

32 **PROPOSITION 3.2.** *Laplace random error. Assume that the noise term ϵ follows a
 33 Laplace distribution*

$$34 \quad (3.9) \quad \epsilon \sim \frac{1}{2b_0} \exp\left(-\frac{|\epsilon|}{b_0}\right) \quad 35 \quad 36$$

37 which has mean 0 and variance $2b_0^2$. Denote $c = \frac{a_*}{\sqrt{\sigma_0^2 + \sigma_*^2}}$ and $b = \frac{b_0}{\sigma_*}$. Then the minimax MSE
 38 of l_1 -LAD is $\tau_*^2 M^*(\epsilon)$, where τ_*^2 (together with c) is determined by the equations
 39

$$40 \quad (3.10) \quad \begin{cases} \tau_*^2 = \left(2b_0^2 + \frac{\tau_*^2 M^*(\epsilon)}{\delta}\right) B(b, c), \\ \frac{\tau_* M^*(\epsilon)}{\delta} = D(b, c), \end{cases} \quad 41 \quad 42 \quad 43 \quad 44$$

45 where

$$46 \quad (3.11) \quad B(b, c) = \frac{1}{D(b, c)} + \frac{N(b, c) + c^2(1 - D(b, c))}{D(b, c)^2(1 + 2b^2)}, \quad 47 \quad 48$$

$$49 \quad D(b, c) = \Phi(c) - \Phi(-c) + f_1(b, c) - f_2(b, c), \quad 48 \quad 49$$

$$50 \quad N(b, c) = (c^2 - 1)(f_1(b, c) - f_2(b, c)) - 2bc(f_1(b, c) + f_2(b, c)) - 2c\Phi(c), \quad 50 \quad 51$$

$$f_1(b, c) = \exp\left\{\frac{1}{2}\left(\frac{1}{b^2} + \frac{2c}{b}\right)\right\} \Phi\left(-c - \frac{1}{b}\right),$$

$$f_2(b, c) = \exp\left\{\frac{1}{2}\left(\frac{1}{b^2} - \frac{2c}{b}\right)\right\} \Phi\left(c - \frac{1}{b}\right).$$

In the classical statistical theory for p fixed and $n \rightarrow \infty$, it is well known that MLE based LAD loss is optimal for Laplace errors. Actually, from (2.21) and (2.22), we obtain that as $\delta \rightarrow \infty$, l_1 -LAD $M(\delta, \epsilon) \rightarrow \frac{\sigma_0^2 M^*(\epsilon)}{4\varphi(0)}$, where $\varphi(x)$ is the density function of ϵ/σ_0 . Comparing it to (3.5), we conclude that, in contrast to LASSO, the minimax MSE of l_1 -LAD is larger for normal error but smaller for Laplace distribution error. It is interesting to see that this conclusion is independent of the choice of the denoiser. Because from the fixed-point equations (2.17) and (2.18), different denoisers lead to different $\eta(\cdot)$ function, and thus different $M^*(\epsilon)$ but the result of τ_* will not be affected if δ is large enough.

But the above conclusion is no longer true in the regime when p is large and comparable to n . Specifically, our numerical studies in Section 4 show that, in this regime, the results depend on δ . For very small δ , LASSO is better than l_1 -LAD; but as δ increases, l_1 -LAD eventually outperforms LASSO and yields smaller MSE. This observation is due to the extra Gaussian noise $\sigma_* Z$ which is dominant over ϵ at very small δ and can be negligible comparing to ϵ when δ is large enough.

PROPOSITION 3.3. *Gaussian mixture random error. Assume that the noise term ϵ follows a mixture of two component Gaussian distribution $\epsilon \sim \epsilon_1 N(0, \sigma_1^2) + \epsilon_2 N(0, \sigma_2^2)$ with $\epsilon_1 + \epsilon_2 = 1$. Denote $c_1 = a_*/\sigma_1$ and $c_2 = a_*/\sigma_2$. Then the minimax MSE of l_1 -LAD is $\tau_*^2 M^*(\epsilon)$, where τ_*^2 (together with c_1 and c_2) is determined by the equations*

$$(3.9) \quad \begin{cases} \tau_*^2 = \frac{\epsilon_1(\sigma_*^2 + \sigma_1^2) f_b(c_1) + \epsilon_2(\sigma_*^2 + \sigma_2^2) f_b(c_2)}{\{\epsilon_1(2\Phi(c_1) - 1) + \epsilon_2(2\Phi(c_2) - 1)\}^2}, \\ \frac{\tau_* M^*(\epsilon)}{\delta} = \epsilon_1(2\Phi(c_1) - 1) + \epsilon_2(2\Phi(c_2) - 1), \end{cases}$$

where

$$f_b(c) = 2\Phi(c) - 1 + 2c\{\epsilon\Phi(-c) - \phi(c)\}.$$

There is no closed form solution for τ_*^2 and we have to use numerical methods. In Section 4, we have also performed extensive numerical studies to compare minimax MSE of l_1 -LAD with LASSO for Gaussian mixture distributed ϵ .

3.3. Penalized Huber's regression. The phase transition and minimax risk of l_1 -penalized Huber's regression can be studied using the same procedure as we did for l_1 -LAD. The following theorem shows that the same phase transition also occurs in l_1 -Huber regression for both noiseless and noisy cases. This phase transition boundary is exactly $\delta = \delta_c(\epsilon)$.

THEOREM 3.3. *Under Assumptions 1, 2 and 4, denote $\hat{\beta}$ the estimator from (2.1) based on the Huber loss. For any $\delta > \delta_c(\epsilon)$, by tuning the parameter λ , we can have $\lim_{p \rightarrow \infty} \frac{1}{p} \|\hat{\beta} - \beta_0\|^2 = 0$ almost surely. Thus we can make consistent estimation for the original signal β_0 in this region. For any $\delta < \delta_c(\epsilon)$, we have $\lim_{p \rightarrow \infty} \frac{1}{p} \|\hat{\beta} - \beta_0\|^2 > 0$ almost surely for any tuning parameter λ . Thus the consistent estimation in this region fails.*

We have the following theorem in the presence of measurement noise, that is, $\sigma_0^2 \neq 0$.

1 THEOREM 3.4. *Under Assumptions 1–4 with the condition of bounded second moment*
 2 *for p_{β_0} in Assumption 2 removed, recall that $M(\delta, \epsilon)$ denotes the minimax MSE of l_1 -Huber.*
 3 *Then, for any $\delta > \delta_c(\epsilon)$, $M(\delta, \epsilon)$ is bounded; for any $\delta < \delta_c(\epsilon)$, $M(\delta, \epsilon)$ is unbounded.*

4
 5 For a given δ, ϵ satisfying $\delta > \delta_c(\epsilon)$, we can estimate the corresponding minimax risk of
 6 l_1 -Huber. The results depend on δ as well as the form of the error distribution p_ϵ . We have
 7 derived the explicit formulas under three different error distributions: normal, Laplace and
 8 Gaussian mixture. The following proposition shows the result for normal error.

9
 10 PROPOSITION 3.4. *Denote $c_0 = \frac{(1+a_*)\gamma}{\sqrt{\sigma_0^2 + \sigma_*^2}}$. Assume that the noise term ϵ follows a normal*
 11 *distribution $\epsilon \sim N(0, \sigma_0^2)$. Then for $\delta > \delta_c(\epsilon)$, the minimax MSE of l_1 -Huber is*

12
 13 (3.10)
$$M(\delta, \epsilon) = \frac{\sigma_0^2 F(c_0) M^*(\epsilon)}{1 - F(c_0) M^*(\epsilon) / \delta},$$

14 where $F(c_0)$ is defined in (3.7) and $\frac{a_*}{1+a_*} (2\Phi(c_0) - 1) = \frac{M^*(\epsilon)}{\delta}$.

15
 16 Comparing (3.10) with (3.6) and (3.5), it can be shown that, for normal random error, the
 17 minimax of MSE l_1 -Huber is less than l_1 -LAD but larger than LASSO due to the fact that
 18 $F(c)$ is decreasing with c and $F(c) \geq 1$. The minimax MSE formulas of l_1 -Huber for Laplace
 19 and Gaussian mixture errors are complicated but the derivation is very straightforward and
 20 similar to the ones for l_1 -LAD. To save space, we will not show the details here.

21
 22
 23
 24 3.4. *Technical novelties.* Since the least squares loss is strongly convex and the LAD
 25 and Huber losses are not, our main results in Section 2 cannot be seen as a straightforward
 26 extension of the results in [4] for LASSO research. For example, the proof of Theorem 2.1
 27 is much more sophisticated than the proof of the corresponding LASSO result in [4], and
 28 requires nontrivial extensions. The main reason is that, according to (2.13), the least square
 29 loss can lead to a constant a_t , and thus a strictly concave function $\tau^2 \mapsto V(\tau^2, \alpha\tau)$. This
 30 substantially simplify the convergence analysis of the SE. On contrary, for LAD and Huber
 31 losses, a_t is not constant and the form of $\tau^2 \mapsto V(\tau^2, \alpha\tau)$ is quite complicated and not con-
 32 cave. As a consequence, the proof of the SE convergence for GAMP is much more difficult
 33 than for AMP. To overcome this difficulty, as suggested by one reviewer, we first construct
 34 a modified GAMP procedure by appropriately fixing certain parameters throughout the iter-
 35 ation to the final values they will converge to. Then, instead of using concavity, we prove
 36 the convergence of τ_t by exploring the large τ^2 behavior of $V(\tau^2, \alpha\tau)$. An addition level of
 37 complexity due to nonstrongly convex loss comes from the proof of Lemma S2. For example,
 38 (S1) can be obtained immediately for strongly convex loss $\rho(\cdot)$ as shown in [12]. However,
 39 for nonstrongly convex loss, we have to develop new techniques in Lemma S1 to prove it.
 40 Moreover, in Section 3, we study the phase transition phenomenon of the penalized robust
 41 estimators. Some techniques used in the proofs of Theorems 3.1–3.3 are outside the scope of
 42 current AMP results. To the best of our knowledge, all previous rigorous analyses of phase
 43 transition were for the case of least square loss.

44
 45 **4. Numerical results.**

46
 47 4.1. *Comparison between theoretical prediction and simulation on finite-size systems.* In
 48 this section, we conduct Monte Carlo simulations to test the validity of our analytical esti-
 49 mation and to determine the finite-size effect. We first confirm that our theoretical results
 50 presented in Sections 2 and 3 are reliable. For this purpose, we focus on the comparison of

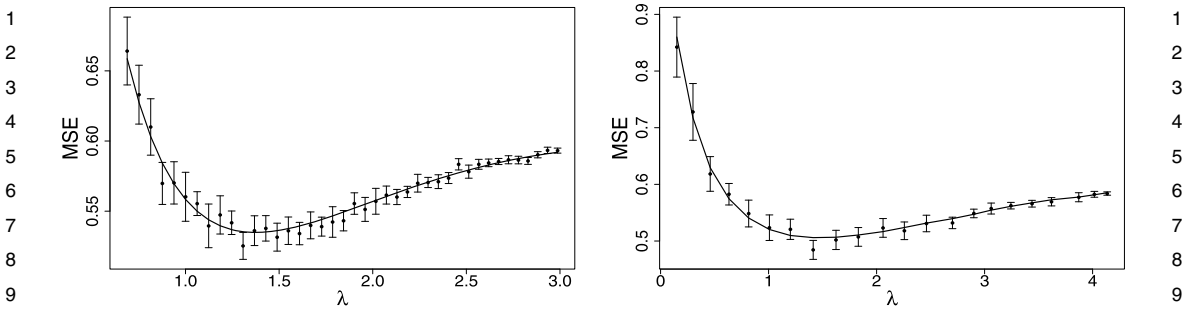


FIG. 2. Comparison between theoretical estimation and simulation study for the change of MSE against tuning parameter λ . Here, $\mu = 2$, $\delta = 0.5$, $\epsilon = 0.15$. The error term follows a Laplace distribution with mean 0 and variance 1. The simulation is based on $p = 1000$ and each setting was repeated 100 times. The solid curve represents the theoretical estimation and the error bars represent the mean and 95% confidence interval summarized over 100 simulated data. Left panel: l_1 -LAD. Right panel: l_1 -Huber with $\gamma = 1$.

the estimated MSE from theory and the MSE computed from numerical algorithms for finite system. We consider two methods: l_1 -LAD and l_1 -Huber. The errors follow a Laplace distribution. The supplementary material contains more simulation results with other types of error distributions.

For each setting, we first found the fixed point of the state evolution for τ_\star^2 by numerically solving (2.28) with the corresponding p_{β_0} . Then using Theorem 2.1 and (2.18), we obtain that $\text{MSE} = \delta\sigma_\star^2$. The comparisons between theoretical estimation and Monte Carlo simulation for MSE of l_1 -LAD are shown in the left panel of Figure 2. We fix the undersampling and sparsity parameters as $\delta = 0.5$ and $\epsilon = 0.15$. The signal is assumed to follow a three-point distribution $p_{\beta_0} \sim (1 - \epsilon)\delta_0 + \frac{\epsilon}{2}\delta_\mu + \frac{\epsilon}{2}\delta_{-\mu}$ with $\mu = 2$. The change of MSE as a function of tuning parameter λ is plotted. The dimension of the simulated data $p = 1000$ and we repeat simulation 100 times for each parameter setting. The mean and standard errors over 100 replications are presented. We use R package *quantreg* to fit the l_1 -LAD estimators. Our analytical curves (solid lines) show a fairly good agreement with the direct computations from numerical algorithms (error bar) for simulated data. Thus our analytical formulas provide reliable estimates for moderate system sizes.

The comparisons between theoretical estimation and Monte Carlo simulation for MSE of l_1 -Huber with $\gamma = 1$ are shown in the right panel of Figure 2. We use the same parameter settings as we did for l_1 -LAD. We use R package *hqreg* to solve the l_1 -Huber optimization problem. Similar to l_1 -LAD, we obtain fairly good agreement between analytic estimation and simulation study for l_1 -Huber as well.

4.2. Phase transition. For the noiseless case, we compare the theoretical phase transition with the empirical one estimated by applying the l_1 -LAD algorithm to simulated data. We first fix a grid of 30 δ values between 0.05 and 1. For each δ , we consider a series of ϵ values between $\epsilon_c(\delta) - 0.1$ and $\epsilon_c(\delta) + 0.1$, where $\epsilon_c(\delta) = \{\epsilon : \delta_c(\epsilon) = \delta\}$. We then have a grid of δ , ϵ values in parameter space $[0, 1]^2$. At each δ , ϵ , we generate 20 problem instances (\mathbf{X}, β_0) with size $p = 1000$. Then $\mathbf{y} = \mathbf{X}\beta_0$. For the i th problem instance, we obtain an output $\hat{\beta}_i$ by using the l_1 -LAD regression method to the i th simulated data with λ chosen to minimize the MSE. We set the success indicator variable $S_i = 1$ if $\frac{\|\hat{\beta}_i - \beta_0\|_2}{\|\beta_0\|_2} \leq 10^{-4}$ and $S_i = 0$ otherwise.

Then at each (δ, ϵ) combination, we have $S = \sum_{i=1}^{20} S_i$.

We analyze the simulated dataset to estimate the phase transition. At each fixed value of δ in our grid, we model the dependence of S on ϵ using logistic regression. We assume that S follows a binomial $B(\pi, 20)$ distribution with $\text{logit}(\pi) = a + b\epsilon$. We define the phase

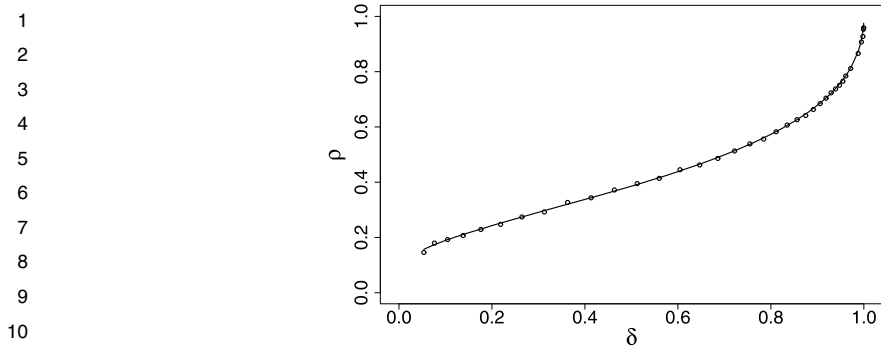


FIG. 3. Observed phase transition for l_1 -LAD in the plane (δ, ρ) . Solid curve represents the theoretical result and circle points represent estimation from simulated data on finite-size systems with $p = 1000$.

transition as the value of ϵ at which the success probability $\pi = 0.5$. In terms of the fitted parameters \hat{a}, \hat{b} , we have the estimated phase transition $\hat{\epsilon}(\delta) = -\hat{a}/\hat{b}$. Figure 3 shows that the agreement between the estimated phase transition curve based on the simulated finite-size systems and the analytical curve based on asymptotic theorem is remarkably good. Note that here we follow Donoho–Tanner notation and plot $\rho = \epsilon/\delta$, the number of nonzero elements in the signal per measurement, as a function of δ .

Figure 4 displays the average MSE of l_1 -LAD over 20 replications as a function of ϵ at 3 different δ values. It is apparent that MSE closes to zero for ϵ below the critical value $\epsilon_c(\delta)$ and is nonzero for ϵ above the critical value $\epsilon_c(\delta)$. Therefore, we can get exact reconstruction for below but not for above.

Figure 5 shows the location of the noise sensitivity boundary $\rho_c(\delta) = \epsilon_c(\delta)/\delta$ as well as the level lines of $M(\delta, \epsilon)$ for $\rho < \rho_c(\delta)$. The different contour lines show positions in the δ, ρ plane where a given minimax MSE is achieved. It is apparent that the MSE increases dramatically as one approaches the phase boundary. Above $\rho_c(\delta)$, the l_1 -LAD MSE is not uniformly bounded.

4.3. *Minimax risk.* In the noisy case, for fixed (δ, ϵ) with $\delta > \delta_c(\epsilon)$, we compare the estimated minimax risk among different regression methods. Figure 6 displays the estimated minimax MSE based on three different regression methods for errors following standard norm, Laplace and mixture of two component Gaussian distributions. The change of minimax MSE as a function of δ for fixed ϵ is plotted.

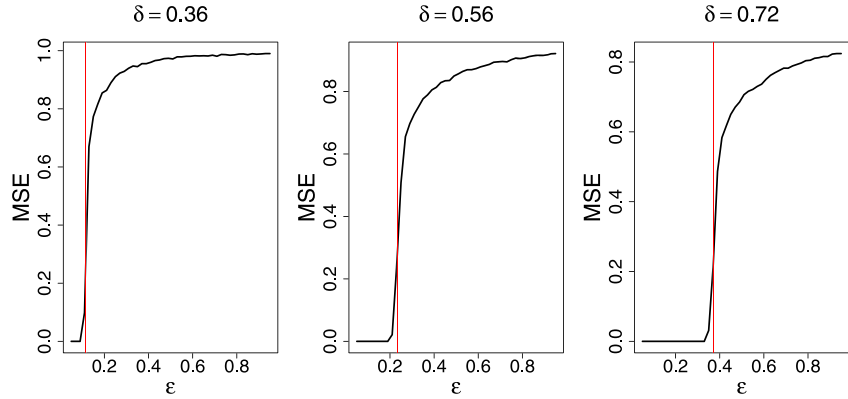


FIG. 4. Empirical average MSE over 20 replications as a function of ϵ at fixed δ for l_1 -LAD regression on simulated noiseless data. The red vertical lines represent the critical ϵ values at the corresponding δ which is equal to $\epsilon_c(\delta)$.

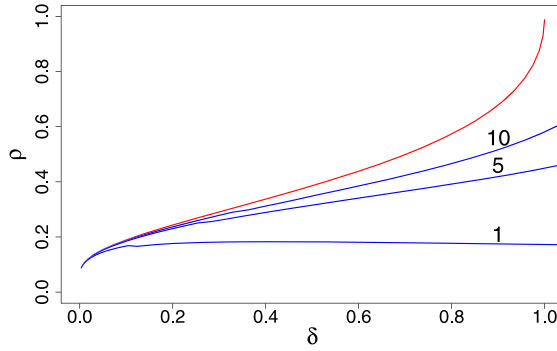


FIG. 5. Phase diagram for the l_1 -LAD regression method in the plane (δ, ρ) for noisy case. Red line: The phase transition boundary $\rho = \rho_c(\delta)$. Blue lines: Level curves for the l_1 -LAD minimax risk $M(\delta, \epsilon)$. Notice that $M(\delta, \epsilon) \rightarrow \infty$ as $\rho \rightarrow \rho_c(\delta)$.

The left panel of Figure 6 shows that for normally distributed random error, LASSO (blue curve) gives the smallest minimax MSE at all δ values. But for Laplace or Gaussian mixture distributed errors, LASSO is not the best. As illustrated in the middle panel of Figure 6 for Laplace distributed error, LASSO gives smaller minimax MSE than l_1 -LAD (red curve) at very small δ value. When δ increases, l_1 -LAD eventually exceeds LASSO and yields smaller minimax MSE. Therefore, the optimal loss is not always the negative log likelihood function in high-dimensional regime. Similar situations happen to Gaussian mixture distributed random error as illustrated in the right panel of Figure 6. The performance of l_1 -penalized Huber's regression (black curve) depends on the parameter γ . Here, for $\gamma = 1$, it gives the smallest minimax MSE at all δ values for Gaussian mixture distributed error. For other two error distributions, its performance is in between. Actually l_1 -penalized Huber's regression can always achieve the best performance if we tune the parameter γ optimally. It is because that Huber's regression is indeed a hybrid of quantile regression and least square regression.

The numerical results shown in Figure 6 are consistent with our theoretical findings in Section 2. Theorem 2.2 indicates that the observed errors follow a mixture of two component distribution including the original error component ϵ and an extra Gaussian component $\sigma_* Z$. Therefore, classical MLE estimation constructed based on the original error distribution cannot always achieve the best performance especially in situations when $\delta \ll 1$. For example, the middle panel of Figure 6 illustrates that LASSO gives a smaller MSE than MLE based l_1 -LAD when $\delta < 0.2$ even if the error actually follows a Laplace distribution. This phenomenon cannot be explained by classical concepts. But if δ is large enough, l_1 -LAD is eventually optimal which is consistent with the classical large n fixed p asymptotic theory.

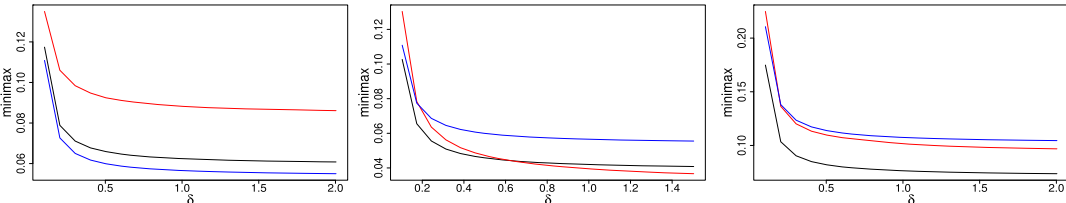


FIG. 6. Minimax MSE as a function of δ at fixed $\epsilon = 0.01$. The blue, red and black lines represent the estimation from LASSO, l_1 -LAD and l_1 -Huber ($\gamma = 1$), respectively. Left panel: standard normal distributed error. Middle panel: Laplace distributed error with mean 0 and variance 1. Right panel: Gaussian mixture distributed error with $\epsilon \sim 0.9N(0, 1) + 0.1N(0, 10)$.

1 Our numerical results provide some guidelines for statisticians to decide among different
 2 loss functions given the noise density. Although appropriately tuning Huber's regression is
 3 the best in all situations, it is often computationally expensive to find the optimal γ in practice.
 4 Therefore, based on our simulation studies, for normal noise, we recommend LASSO; for
 5 heavy tailed errors such as exponential ones, we recommend l_1 -LAD for large δ and LASSO
 6 for small δ ; for mixture of Gaussian errors, we recommend l_1 -Huber.
 7

8 **5. Discussion.** In this paper, we study the asymptotic MSE of l_1 -penalized robust es-
 9 timators in the framework of GAMP algorithm under high-dimensional asymptotics where
 10 the number of parameters p and the number of observations n are both tending to infinity,
 11 at the same rate. Our analysis shows the existence of a sharp phase transition in the
 12 two-dimensional (δ, ϵ) plane which is consistent with the phase transition in LASSO. The
 13 analytical calculations are compared with numerical simulations on finite-size systems and
 14 the agreement between the data analysis and theoretical prediction is fairly good, and thus,
 15 our formulas are validated. Our numerical studies show that when δ is small enough, least
 16 squares loss becomes preferable to LAD loss for Laplace errors. Therefore, the most optimal
 17 loss function is no longer the negative log likelihood function. This is because of the extra
 18 Gaussian component caused by high-dimensional asymptotics. This new phenomenon was
 19 first discovered in [18] and later confirmed in [12] for robust regression. We show here that
 20 this phenomenon can be characterized rigorously using GAMP techniques for penalized ro-
 21 bust regression as well. Our results can be applied to the case of $k \log(p)/n \rightarrow 0$ in practice
 22 by letting $\delta \rightarrow \infty$ or $\epsilon \rightarrow 0$. As shown by Figure S6 in the supplementary material, we can
 23 obtain fairly good agreement between analytic estimation and simulation study in the case of
 24 small $k \log(p)/n$ with $n < p$.
 25

26 The focus of this paper is on mathematical analysis of the l_1 -penalized robust regression
 27 methods. The analytical predictions are derived based on given signal distribution p_{β_0} and
 28 error distribution p_ϵ . However, in practice, these quantities are usually unknown. As shown
 29 in [10], even for LASSO, the loss of estimator is hard to estimate based on the data set. There
 30 has been some recent work for the case of LASSO that uses Stein's Unbiased Risk Estimator
 31 (SURE) to propose unbiased predictions of the risk without using signal distribution p_{β_0} ;
 32 see, for example, [1, 23]. Interesting areas for the future include following that direction to
 33 provide analytical predictions in real data analysis based on robust estimators.
 34

35 In additional to the l_1 -penalization, [14] studied the phase transitions of regularized least
 36 square estimators under a wide range of penalizations. Krzakala [21] proposed a probabilistic
 37 approach to reconstruct the signal by assuming that the signals follow a parametric Gauss-
 38 Bernoulli distribution. Then they add an expectation maximization based procedure to learn
 39 the unknown distribution parameters. The phase diagram of this model has also been an-
 40 alyzed and compared with the result based on l_1 -penalization. One of our future research
 41 topics is to study the phase transition of regularized robust regression under other types of
 42 penalizations.
 43

44 An important assumption made for deriving the asymptotic result in GAMP is that the
 45 matrix \mathbf{X} has i.i.d. Gaussian entries. The reason is that the rigorous proof for SE of GAMP
 46 can only be given for this class of matrices although simulation studies have shown that the
 47 results hold for a much broader class of matrices. For least square loss, the SE is proved
 48 in [2] under i.i.d. sub-Gaussian matrices. [20] has derived the asymptotic result of LASSO
 49 estimators under general Gaussian matrices using nonrigorous replica method. Our another
 50 future direction is to rigorously prove this result using the method developed in [6]. For this
 51 purpose, the main challenge is to find conditions for \mathbf{X} under which the GAMP can converge
 52 to those fixed points.
 53

APPENDIX A: PROOF OF THEOREM 3.1

PROOF. For $\sigma_0^2 = 0$, denote $c = \frac{a_\star}{\sigma_\star}$ and $\hat{Z} = \frac{\tilde{Z}}{\sigma_\star}$. Then the fixed-point equation (2.28) becomes

$$(A.1) \quad \tau_\star^2 = V(\tau_\star^2, \alpha\tau_\star) = \sigma_\star^2 F(c),$$

where $F(c)$ is defined in (3.7) and c is determined through

$$(A.2) \quad P(|\hat{Z}| \leq c) = \pi_\star = 2\Phi(c) - 1.$$

It can be shown that $F(c)$ is a decreasing function with $F(0) = \pi/2$ and $F(\infty) = 1$.

As shown in the proof of Proposition 2.3, $V(\tau^2, \alpha\tau) < \tau^2$ as $\tau \rightarrow \infty$. We argue that if the only fixed point satisfies $\tau_\star^2 = 0$, it must be true that the derivative of $V(\tau^2, \alpha\tau)$ at $\tau^2 = 0$ is smaller than or equal to 1. That is,

$$\frac{dV(\tau^2, \alpha\tau)}{d\tau^2} \Big|_{\tau^2=0} \leq 1$$

for appropriately chosen α . Starting from (A.1), we obtain

$$\frac{dV(\tau^2, \alpha\tau)}{d\tau^2} \Big|_{\tau^2=0} = \frac{d\sigma^2}{d\tau^2} \Big|_{\tau^2=0} F(c(\tau)) + \sigma_\star^2 F'(c(\tau)) \frac{dc(\tau)}{d\tau^2} \Big|_{\tau^2=0}.$$

Note that

$$(A.3) \quad \pi_\star = \frac{1}{\delta} E\{\Phi(-\alpha + w_\star) + \Phi(-\alpha - w_\star)\},$$

where $w_\star = \frac{\beta_0}{\tau}$. Taking derivative on both side of (A.2), we have

$$2\phi(c) \frac{dc}{d\tau^2} = \frac{1}{\delta} E\left\{-\frac{w_\star}{2\tau^2\delta} [\phi(-\alpha + w_\star) - \phi(-\alpha - w_\star)]\right\} \xrightarrow{\tau^2 \rightarrow 0} 0.$$

Therefore, $\frac{dc(\tau)}{d\tau^2} \Big|_{\tau^2=0} = 0$ and for $p_{\beta_0} \in \mathcal{F}$,

$$(A.4) \quad \begin{aligned} \frac{dV(\tau^2, \alpha\tau)}{d\tau^2} \Big|_{\tau^2=0} \\ = \{\epsilon(1 + \alpha^2) + (1 - \epsilon)[2(1 + \alpha^2)\Phi(-\alpha) - 2\alpha\phi(\alpha)]\} \frac{F(c)}{\delta}, \end{aligned}$$

where we have used (S2). Denote $\delta_{\min}(\epsilon)$ the smallest δ for a fixed ϵ such that

$$(A.5) \quad \min_{\alpha \geq 0} \left\{ \frac{dV(\tau^2, \alpha\tau)}{d\tau^2} \Big|_{\tau^2=0} \right\} \leq 1.$$

The terms inside $\{\cdot\}$ on the right-hand side of (A.4) are minimized when we choose $\alpha = \alpha_c$ such that

$$(A.6) \quad \epsilon = 1 - \frac{\alpha_c}{\alpha_c - 2\alpha_c\Phi(-\alpha_c) + 2\phi(\alpha_c)}.$$

Then if we take

$$(A.7) \quad \delta_{\min}(\epsilon) = \frac{2\phi(\alpha_c)}{\alpha_c - 2\alpha_c\Phi(-\alpha_c) + 2\phi(\alpha_c)},$$

we can show that the second term $F(c)$ on the right-hand side of (A.4) is also minimized at this value. Toward this end, substituting (A.6) and (A.7) into (A.3), we get

$$\pi_\star \xrightarrow{\tau^2 \rightarrow 0} \frac{\epsilon + 2(1 - \epsilon)\Phi(-\alpha_c)}{\delta_{\min}(\epsilon)} = 1.$$

1 Therefore, from (A.2), we have $c = \infty$, and thus $F(c) = 1$ which is also the smallest value for
 2 $F(c)$. Therefore, the smallest δ that satisfies (A.5) is just the $\delta_{\min}(\epsilon)$ defined in (A.7) which
 3 is exactly equal to the $\delta_c(\epsilon)$ defined in (3.1).

4 Next, we prove that if $\delta > \delta_c(\epsilon)$, we have $V(\tau^2, \alpha_c \tau) < \tau^2$ for any $\tau^2 > 0$. Thus the unique
 5 fixed-point solution is $\tau^2 = 0$. For $p_{\beta_0} \in \mathcal{F}_\epsilon$, (S2) can be written as

$$\begin{aligned} \sigma^2 &= \frac{\tau^2}{\delta} \{ (1 - \epsilon) \{ 2(1 + \alpha^2) \Phi(-\alpha) - 2\alpha\phi(\alpha) \} + \epsilon(1 + \alpha^2) \\ &\quad + \epsilon E \{ (1 + \alpha^2 - w_\star^2) [\Phi(-\alpha - w_\star) - \Phi(\alpha - w_\star)] \\ &\quad - (\alpha + w_\star)\phi(\alpha - w_\star) - (\alpha - w_\star)\phi(\alpha + w_\star) \} \}. \end{aligned}$$

12 Plug in (A.6), we obtain

$$(A.8) \quad \sigma^2 = \frac{\tau^2}{\delta} \{ \delta_c(\epsilon) + \epsilon E \{ \Phi(-\alpha_c - w_\star) - \Phi(\alpha_c - w_\star) \} + \epsilon g(\alpha_c) \},$$

16 where

$$\begin{aligned} g(\alpha) &= (\alpha^2 - w_\star^2) E \{ \Phi(-\alpha - w_\star) - \Phi(\alpha - w_\star) \} \\ &\quad - (\alpha + w_\star) E \{ \phi(\alpha - w_\star) \} - (\alpha - w_\star) E \{ \phi(\alpha + w_\star) \}. \end{aligned}$$

20 Since $g(0) = 0$ and

$$g'(\alpha) = 2\alpha E \{ \Phi(-\alpha - w_\star) - \Phi(\alpha - w_\star) \} - E \{ \phi(\alpha - w_\star) \} - E \{ \phi(\alpha + w_\star) \}$$

23 which is less than 0 for any $\alpha > 0$, therefore, $g(\alpha) < 0$ for any $\alpha > 0$. On the other hand, for
 24 $\alpha = \alpha_c$, from (A.2) and (A.3), we have

$$2\Phi(c) - 1 = \frac{1}{\delta} [\delta_c(\epsilon) + \epsilon E \{ \Phi(-\alpha_c - w_\star) - \Phi(\alpha_c - w_\star) \}].$$

28 From (3.7) and using $c\Phi(-c) < \phi(c)$ for all $c > 0$, we get

$$(A.9) \quad F(c) < \frac{1}{2\Phi(c) - 1} = \frac{\delta}{\delta_c(\epsilon) + \epsilon E \{ \Phi(-\alpha_c - w_\star) - \Phi(\alpha_c - w_\star) \}}.$$

32 Combining it to (A.1), (A.8) and the fact that $g(\alpha) < 0$, we obtain

$$(A.10) \quad V(\tau^2, \alpha_c \tau) = \sigma^2 F(c) < \tau^2$$

35 for any $\tau^2 > 0$. \square

APPENDIX B: PROOF OF THEOREM 3.2

40 PROOF. From Theorem 2.1, we have

$$M(\delta, \epsilon) = \min_{\alpha} \sup_{p_{\beta_0} \in \mathcal{F}_\epsilon} E \{ \|\eta(\beta_0 + \tau_\star Z; \alpha \tau_\star) - \beta_0\|^2 \}.$$

44 Since the class \mathcal{F}_ϵ is invariant by rescaling, the worst case MSE must be proportional to the
 45 only scale in the problem, that is, τ_\star^2 . We get

$$M(\delta, \epsilon) = \tau_\star^2 M^*(\epsilon),$$

48 where

$$(B.1) \quad M^*(\epsilon) = \min_{\alpha} \sup_{p_{w_\star} \in \mathcal{F}_\epsilon} E [\eta(w_\star + Z, \alpha) - w_\star]^2,$$

1 where $w_\star = \beta_0/\tau_\star$. Minimax MSE of soft thresholding was studied in [15, 17, 33] where one
 2 can find a considerable amount of information about the behavior of the optimal threshold α
 3 and the least favorable distribution $p_{\beta_0} \in \mathcal{F}_\epsilon$. Particularly, the supremum is achieved only by
 4 a three-point mixture on the centered real line $\mathbb{R} \cup \{-\infty, \infty\}$:

$$5 \quad (B.2) \quad p_{\beta_0} = \frac{\epsilon}{2} \delta_{+\infty} + (1 - \epsilon) \delta_0 + \frac{\epsilon}{2} \delta_{-\infty}. \quad 5 \\ 6$$

7 Then the explicit formula of $M^\star(\epsilon)$ takes the form

$$8 \quad M^\star(\epsilon) = \min_{\alpha} \{ \epsilon(1 + \alpha^2) + (1 - \epsilon)[2(1 + \alpha^2)\Phi(-\alpha) - 2\alpha\phi(\alpha)] \} \quad 8 \\ 9 \\ 10 \quad (B.3) \quad = \frac{2\phi(\alpha_c)}{\alpha_c + 2(\phi(\alpha_c) - \alpha_c\Phi(-\alpha_c))} = \delta_c(\epsilon), \quad 10 \\ 11$$

12 where α_c is defined in (3.2). Therefore, the finiteness of $M(\delta, \epsilon)$ depends on τ_\star which is the
 13 solution of fix-point equation $\tau^2 = V(\tau^2, \alpha_c \tau)$.

14 For $\sigma_0^2 \neq 0$, it is apparent that $V(\tau^2, \alpha_c \tau)|_{\tau^2=0} > 0$. Thus, we can get finite solution for
 15 equation $\tau^2 = V(\tau^2, \alpha_c \tau)$ if $V(\tau^2, \alpha_c \tau) < \tau^2$ for large enough τ^2 . Let us first determine the
 16 phase transition curve by finding the smallest δ such that $V(\tau^2, \alpha_c \tau) < \tau^2$ as $\tau^2 \rightarrow \infty$ for
 17 fixed ϵ .

18 From (S2), we have that $\tau^2 \rightarrow \infty$ leads to $\sigma^2 \rightarrow \infty$ and $\hat{Z} \rightarrow N(0, 1)$. In this situation,
 19 $V(\tau^2, \alpha_c \tau)$ takes the form

$$21 \quad (B.4) \quad V(\tau^2, \alpha_c \tau) \rightarrow \frac{\tau^2 M^\star(\epsilon)}{\delta} F(c) \leq \frac{\tau^2 M^\star(\epsilon)}{\delta(2\Phi(c) - 1)}, \quad 21 \\ 22$$

23 where the second step is obtained using (A.9) and the equality only holds for $c = \infty$. From
 24 (S3), we get

$$25 \quad (B.5) \quad 2\Phi(c) - 1 = \frac{1}{\delta} \{ \epsilon + 2(1 - \epsilon)\Phi(-\alpha) \} \quad 25 \\ 26$$

27 as $\tau_\star \rightarrow \infty$. If we plug in the optimal α from (3.2), we have

$$29 \quad (B.6) \quad 2\Phi(c) - 1 = \frac{1}{\delta} \frac{2\phi(\alpha_c)}{\alpha_c + 2(\phi(\alpha_c) - \alpha_c\Phi(-\alpha_c))} = \frac{M^\star(\epsilon)}{\delta}. \quad 29 \\ 30$$

31 For fixed ϵ , plugging it into (B.4), we have $V(\tau^2, \alpha_c \tau) \leq \tau^2$ for large enough τ^2 if $\delta \leq$
 32 $\delta_c(\epsilon) = M^\star(\epsilon)$. If $\delta > \delta_c(\epsilon)$, we can strictly have $V(\tau^2, \alpha_c \tau) < \tau^2$ as $\tau^2 \rightarrow \infty$ and thus at
 33 least one finite solution τ_\star^2 for the fix-point equation which leads to a finite minimax MSE.

34 On the other hand, if $\delta < \delta_c(\epsilon)$, we can prove that $V(\tau^2, \alpha_c \tau) > \tau^2$ for any $\tau \geq 0$, thus the
 35 only solution is $\tau_\star^2 = \infty$ which leads to an infinite minimax MSE. Toward this end, we start
 36 from

$$37 \quad V(\tau^2, \alpha_c \tau) = E\{G(\tilde{Z}, a)^2\}, \quad 37 \\ 38$$

39 where $\tilde{Z} = \varepsilon + \sigma Z$ which can be described as $\tilde{Z} = F_\varepsilon \star N(0, \sigma^2)$ (here \star denotes convolution).
 40 Denote $\xi_{\tilde{Z}}$ the score function for location of \tilde{Z} , then using (2.19) we have $1 = |E_{\tilde{Z}} G'| =$
 41 $|E_{\tilde{Z}} G \xi_{\tilde{Z}}|$. Meanwhile, by Cauchy–Schwarz, $|E_{\tilde{Z}} G \xi_{\tilde{Z}}| \leq \sqrt{E_{\tilde{Z}} G^2} \sqrt{E_{\tilde{Z}} \xi_{\tilde{Z}}^2}$. We conclude that

$$43 \quad V(\tau^2, \alpha_c \tau) \geq \frac{|E_{\tilde{Z}} G \xi_{\tilde{Z}}|^2}{E_{\tilde{Z}} \xi_{\tilde{Z}}^2} = \frac{|E_{\tilde{Z}} G'|^2}{E_{\tilde{Z}} \xi_{\tilde{Z}}^2} = \frac{1}{I(\tilde{Z})}, \quad 43 \\ 44$$

45 where $I(\tilde{Z})$ is the Fisher information of $F_{\tilde{Z}}$. From convexity and translation-invariance of
 46 Fisher information $I(\tilde{Z}) = I(F_\varepsilon \star N(0, \sigma^2)) < I(N(0, \sigma^2)) = 1/\sigma^2$ if $\text{var}(\varepsilon) = \sigma_0^2 > 0$.
 47 Therefore,

$$49 \quad (B.7) \quad V(\tau^2, \alpha_c \tau) > \sigma^2(\alpha_c) \stackrel{(a)}{=} \frac{\tau^2 M^\star(\epsilon)}{\delta} = \frac{\tau^2 \delta_c(\epsilon)}{\delta} \quad 49 \\ 50$$

1 which is larger than τ^2 for $\delta < \delta_c(\epsilon)$. In step (a) of (B.7), we have used (2.17), (B.1) and
 2 (B.3). We conclude that the phase transition curve is determined by (B.3), which is exactly
 3 the same as the transition curve (A.6) and (A.7) derived in noiseless case. \square

4
 5 **Acknowledgments.** The author thanks the editor, associate editor and four referees for
 6 many insightful comments and suggestions which have led to great improvement of this
 7 article.

9 SUPPLEMENTARY MATERIAL

10 **Supplement: More simulations and proofs** (DOI: 10.1214/19-AOS1923SUPP; .pdf).
 11 The supplement provides more simulation results and proofs of Theorems 2.2, 3.3, 3.4 as
 12 well as all propositions and lemmas.

14 REFERENCES

- [1] BAYATI, M., ERDOGDU, M. A. and MONTANARI, A. (2013). Estimating LASSO risk and noise level. In *Advances in Neural Information Processing Systems 26* (C. J. C. Burges, L. Bottou, M. Welling, Z. Ghahramani and K. Q. Weinberger, eds.) 944–952. Curran Associates.
- [2] BAYATI, M., LELARGE, M. and MONTANARI, A. (2015). Universality in polytope phase transitions and message passing algorithms. *Ann. Appl. Probab.* **25** 753–822. MR3313755 <https://doi.org/10.1214/14-AAP1010>
- [3] BAYATI, M. and MONTANARI, A. (2011). The dynamics of message passing on dense graphs, with applications to compressed sensing. *IEEE Trans. Inform. Theory* **57** 764–785. MR2810285 <https://doi.org/10.1109/TIT.2010.2094817>
- [4] BAYATI, M. and MONTANARI, A. (2012). The LASSO risk for Gaussian matrices. *IEEE Trans. Inform. Theory* **58** 1997–2017. MR2951312 <https://doi.org/10.1109/TIT.2011.2174612>
- [5] BEAN, D., BICKEL, P. J., EL KAROUI, N. and YU, B. (2013). Optimal M-estimation in high-dimensional regression. *Proc. Natl. Acad. Sci. USA* **110** 14563–14568. <https://doi.org/10.1073/pnas.1307845110>
- [6] BERTHIER, R., MONTANARI, A. and NGUYEN, P. (2017). State evolution for approximate message passing with non-separable functions. CoRR abs/1708.03950.
- [7] BICKEL, P. J., RITOV, Y. and TSYBAKOV, A. B. (2009). Simultaneous analysis of lasso and Dantzig selector. *Ann. Statist.* **37** 1705–1732. MR2533469 <https://doi.org/10.1214/08-AOS620>
- [8] BRADIC, J. (2016). Robustness in sparse high-dimensional linear models: Relative efficiency and robust approximate message passing. *Electron. J. Stat.* **10** 3894–3944. MR3581957 <https://doi.org/10.1214/16-EJS1212>
- [9] BÜHLMANN, P. and VAN DE GEER, S. (2011). *Statistics for High-Dimensional Data: Methods, Theory and Applications*. Springer Series in Statistics. Springer, Heidelberg. MR2807761 <https://doi.org/10.1007/978-3-642-20192-9>
- [10] CAI, T. T. and GUO, Z. (2018). Accuracy assessment for high-dimensional linear regression. *Ann. Statist.* **46** 1807–1836. MR3819118 <https://doi.org/10.1214/17-AOS1604>
- [11] CANDÈS, E. J., ROMBERG, J. K. and TAO, T. (2006). Stable signal recovery from incomplete and inaccurate measurements. *Comm. Pure Appl. Math.* **59** 1207–1223. MR2230846 <https://doi.org/10.1002/cpa.20124>
- [12] DONOHO, D. and MONTANARI, A. (2016). High dimensional robust M-estimation: Asymptotic variance via approximate message passing. *Probab. Theory Related Fields* **166** 935–969. MR3568043 <https://doi.org/10.1007/s00440-015-0675-z>
- [13] DONOHO, D. and TANNER, J. (2009). Observed universality of phase transitions in high-dimensional geometry, with implications for modern data analysis and signal processing. *Philos. Trans. R. Soc. Lond. Ser. A Math. Phys. Eng. Sci.* **367** 4273–4293. With electronic supplementary materials available online. MR2546388 <https://doi.org/10.1098/rsta.2009.0152>
- [14] DONOHO, D. L., JOHNSTONE, I. and MONTANARI, A. (2013). Accurate prediction of phase transitions in compressed sensing via a connection to minimax denoising. *IEEE Trans. Inform. Theory* **59** 3396–3433. MR3061255 <https://doi.org/10.1214/13-2239356>
- [15] DONOHO, D. L. and JOHNSTONE, I. M. (1994). Ideal spatial adaptation by wavelet shrinkage. *Biometrika* **81** 425–455. MR1311089 <https://doi.org/10.1093/biomet/81.3.425>
- [16] DONOHO, D. L., MALEKI, A. and MONTANARI, A. (2009). Message-passing algorithms for compressed sensing. *Proc. Natl. Acad. Sci. USA* **106** 18914–18919. <https://doi.org/10.1073/pnas.0909892106>

1 [17] DONOHO, D. L., MALEKI, A. and MONTANARI, A. (2011). The noise-sensitivity phase transition in compressed sensing. *IEEE Trans. Inform. Theory* **57** 6920–6941. [MR2882271](#) <https://doi.org/10.1109/TIT.2011.2165823>

2 [18] EL KAROUI, N., BEAN, D., BICKEL, P. J., LIM, C. and YU, B. (2013). On robust regression with high-dimensional predictors. *Proc. Natl. Acad. Sci. USA* **110** 14557–14562. [https://doi.org/10.1073/pnas.1307842110](#)

3 [19] HUANG, H. (2020). Supplement to “Asymptotic risk and phase transition of l_1 -penalized robust estimator.” [https://doi.org/10.1214/19-AOS1923SUPP](#)

4 [20] JAVANMARD, A. and MONTANARI, A. (2014). Hypothesis testing in high-dimensional regression under the Gaussian random design model: Asymptotic theory. *IEEE Trans. Inform. Theory* **60** 6522–6554. [MR3265038](#) <https://doi.org/10.1109/TIT.2014.2343629>

5 [21] KRZAKALA, F., MÉZARD, M., SAUSSET, F., SUN, Y. F. and ZDEBOROVÁ, L. (2012). Statistical-physics-based reconstruction in compressed sensing. *Phys. Rev. X* **2** 021005. [https://doi.org/10.1103/PhysRevX.2.021005](#)

6 [22] LAMBERT-LACROIX, S. and ZWALD, L. (2011). Robust regression through the Huber’s criterion and adaptive lasso penalty. *Electron. J. Stat.* **5** 1015–1053. [MR2836768](#) <https://doi.org/10.1214/11-EJS635>

7 [23] MOUSAVI, A., MALEKI, A. and BARANIUK, R. G. (2017). Consistent parameter estimation for LASSO and approximate message passing. *Ann. Statist.* **45** 2427–2454. [MR3737897](#) <https://doi.org/10.1214/16-AOS1529>

8 [24] RANGAN, S. (2011). Generalized approximate message passing for estimation with random linear mixing. In *Information Theory Proceedings (ISIT), 2011 IEEE International Symposium on* 2168–2172. [https://doi.org/10.1109/ISIT.2011.6033942](#)

9 [25] RANGAN, S., SCHNITER, P. and FLETCHER, A. (2014). On the convergence of approximate message passing with arbitrary matrices. In *2014 IEEE International Symposium on Information Theory* 236–240. [https://doi.org/10.1109/ISIT.2014.6874830](#)

10 [26] RANGAN, S., SCHNITER, P. and FLETCHER, A. K. (2017). Vector approximate message passing. In *2017 IEEE International Symposium on Information Theory (ISIT)* 1588–1592.

11 [27] RASKUTTI, G., WAINWRIGHT, M. J. and YU, B. (2011). Minimax rates of estimation for high-dimensional linear regression over ℓ_q -balls. *IEEE Trans. Inform. Theory* **57** 6976–6994. [MR2882274](#) <https://doi.org/10.1109/TIT.2011.2165799>

12 [28] SCHNITER, P., RANGAN, S. and FLETCHER, A. K. (2016). Vector approximate message passing for the generalized linear model. In *2016 50th Asilomar Conference on Signals, Systems and Computers* 1525–1529. [https://doi.org/10.1109/ACSSC.2016.7869633](#)

13 [29] TIBSHIRANI, R. (1996). Regression shrinkage and selection via the lasso. *J. Roy. Statist. Soc. Ser. B* **58** 267–288. [MR1379242](#)

14 [30] VERZELEN, N. (2012). Minimax risks for sparse regressions: Ultra-high dimensional phenomenons. *Electron. J. Stat.* **6** 38–90. [MR2879672](#) <https://doi.org/10.1214/12-EJS666>

15 [31] VILA, J., SCHNITER, P., RANGAN, S., KRZAKALA, F. and ZDEBOROVÁ, L. (2015). Adaptive damping and mean removal for the generalized approximate message passing algorithm. In *2015 IEEE International Conference on Acoustics, Speech and Signal Processing (ICASSP) 2021–2025*. [https://doi.org/10.1109/ICASSP.2015.7178325](#)

16 [32] WANG, L. (2013). The L_1 penalized LAD estimator for high dimensional linear regression. *J. Multivariate Anal.* **120** 135–151. [MR3072722](#) <https://doi.org/10.1016/j.jmva.2013.04.001>

17 [33] ZHANG, C.-H. (2012). Minimax ℓ_q risk in ℓ_p balls. In *Contemporary Developments in Bayesian Analysis and Statistical Decision Theory: A Festschrift for William E. Strawderman. Inst. Math. Stat. (IMS) Collect.* **8** 78–89. IMS, Beachwood, OH. [MR3202504](#) <https://doi.org/10.1214/11-IMSCOLL806>

18 [34] ZHENG, L., MALEKI, A., WENG, H., WANG, X. and LONG, T. (2017). Does ℓ_p -minimization outperform ℓ_1 -minimization? *IEEE Trans. Inform. Theory* **63** 6896–6935. [MR3724407](#) <https://doi.org/10.1109/TIT.2017.2717585>

19 [35] [<author>](#)

20 [36] [<mr>](#)

21 [37] [<mr>](#)

22 [38] [<mr>](#)

23 [39] [<mr>](#)

24 [40] [<mr>](#)

25 [41] [<mr>](#)

26 [42] [<mr>](#)

27 [43] [<mr>](#)

28 [44] [<mr>](#)

29 [45] [<mr>](#)

30 [46] [<mr>](#)

31 [47] [<mr>](#)

32 [48] [<mr>](#)

33 [49] [<mr>](#)

34 [50] [<mr>](#)

35 [51] [<mr>](#)

1 THE ORIGINAL REFERENCE LIST 1
2

3 The list of entries below corresponds to the original Reference section of your article. The bibliography
4 section on previous page was retrieved from MathSciNet applying an automated procedure.
5 Please check both lists and indicate those entries which lead to mistaken sources in automatically generated
6 Reference list.

[1] BAYATI, M., ERDOGDU, M. A. and MONTANARI, A. (2013). Estimating LASSO Risk and Noise Level. In *Advances in Neural Information Processing Systems 26* (C. J. C. Burges, L. Bottou, M. Welling, Z. Ghahramani and K. Q. Weinberger, eds.) 944–952. Curran Associates, Inc., ???.

[2] BAYATI, M., LELARGE, M. and MONTANARI, A. (2015). Universality in polytope phase transitions and message passing algorithms. *Ann. Appl. Probab.* **25** 753–822. <https://doi.org/10.1214/14-AAP1010>

[3] BAYATI, M. and MONTANARI, A. (2011). The Dynamics of Message Passing on Dense Graphs, with Applications to Compressed Sensing. *IEEE Transactions on Information Theory* **57** 764–785. <https://doi.org/10.1109/TIT.2010.2094817>

[4] BAYATI, M. and MONTANARI, A. (2012). The LASSO Risk for Gaussian Matrices. *IEEE Trans. Information Theory* **58** 1997–2017.

[5] BEAN, D., BICKEL, P. J., EL KAROUI, N. and YU, B. (2013). Optimal M-estimation in high-dimensional regression. *Proceedings of the National Academy of Sciences* **110** 14563–14568. <https://doi.org/10.1073/pnas.1307845110>

[6] BERTHIER, R., MONTANARI, A. and NGUYEN, P. (2017). State Evolution for Approximate Message Passing with Non-Separable Functions. *CoRR* **abs/1708.03950**.

[7] BICKEL, P. J., RITOV, Y. and TSYBAKOV, A. B. (2009). Simultaneous analysis of Lasso and Dantzig selector. *Ann. Statist.* **37** 1705–1732. <https://doi.org/10.1214/08-AOS620>

[8] BRADIC, J. (2016). Robustness in sparse high-dimensional linear models: Relative efficiency and robust approximate message passing. *Electron. J. Statist.* **10** 3894–3944. <https://doi.org/10.1214/16-EJS1212>

[9] BHLMANN, P. and VAN DE GEER, S. (2011). *Statistics for High-Dimensional Data: Methods, Theory and Applications*, 1st ed. Springer Publishing Company, Incorporated, ???.

[10] CAI, T. T. and GUO, Z. (2018). Accuracy assessment for high-dimensional linear regression. *Ann. Statist.* **46** 1807–1836. <https://doi.org/10.1214/17-AOS1604>

[11] CANDES, E. J., ROMBERG, J. K. and TAO, T. (2006). Stable signal recovery from incomplete and inaccurate measurements. *Communications on Pure and Applied Mathematics* **59** 1207–1223. <https://doi.org/10.1002/cpa.20124>

[12] DONOHO, D. and MONTANARI, A. (2015). High dimensional robust M-estimation: asymptotic variance via approximate message passing. *Probability Theory and Related Fields* 1–35. <https://doi.org/10.1007/s00440-015-0675-z>

[13] DONOHO, D. and TANNER, J. (2009). Observed universality of phase transitions in high-dimensional geometry, with implications for modern data analysis and signal processing. *Philosophical Transactions of the Royal Society of London A: Mathematical, Physical and Engineering Sciences* **367** 4273–4293. <https://doi.org/10.1098/rsta.2009.0152>

[14] DONOHO, D. L., JOHNSTONE, I. and MONTANARI, A. (2013). Accurate prediction of phase transitions in compressed sensing via a connection to minimax denoising. *IEEE transactions on information theory* **59** 3396–3433.

[15] DONOHO, D. L. and JOHNSTONE, J. M. (1994). Ideal spatial adaptation by wavelet shrinkage. *Biometrika* **81** 425. <https://doi.org/10.1093/biomet/81.3.425>

[16] DONOHO, D. L., MALEKI, A. and MONTANARI, A. (2009). Message-passing algorithms for compressed sensing. *Proceedings of the National Academy of Sciences* **106** 18914–18919. <https://doi.org/10.1073/pnas.0909892106>

[17] DONOHO, D. L., MALEKI, A. and MONTANARI, A. (2011). The Noise-Sensitivity Phase Transition in Compressed Sensing. *IEEE Transactions on Information Theory* **57** 6920–6941. <https://doi.org/10.1109/TIT.2011.2165823>

[18] EL KAROUI, N., BEAN, D., BICKEL, P. J., LIM, C. and YU, B. (2013). On robust regression with high-dimensional predictors. *Proceedings of the National Academy of Sciences* **110** 14557–14562. <https://doi.org/10.1073/pnas.1307842110>

[19] JAVANMARD, A. and MONTANARI, A. (2014). Hypothesis Testing in High-Dimensional Regression Under the Gaussian Random Design Model: Asymptotic Theory. *IEEE Transactions on Information Theory* **60** 6522–6554. <https://doi.org/10.1109/TIT.2014.2343629>

[20] KRZAKALA, F., MÉZARD, M., SAUSSET, F., SUN, Y. F. and ZDEBOROVÁ, L. (2012). Statistical-Physics-Based Reconstruction in Compressed Sensing. *Phys. Rev. X* **2** 021005. <https://doi.org/10.1103/PhysRevX.2.021005>

1 [21] LAMBERT-LACROIX, S. and ZWALD, L. (2011). Robust regression through the Huber's criterion and adaptive lasso penalty. *Electron. J. Stat.* **5** 1015–1053. 2836768 <https://doi.org/10.1214/11-EJS635>

2 [22] MOUSAVI, A., MALEKI, A. and BARANIUK, R. G. (2017). Consistent parameter estimation for LASSO
3 and approximate message passing. *Ann. Statist.* **45** 2427–2454. <https://doi.org/10.1214/16-AOS1529>

4 [23] RANGAN, S. (2011). Generalized approximate message passing for estimation with random linear mix-
5 ing. In *Information Theory Proceedings (ISIT), 2011 IEEE International Symposium on* 2168–2172.
6 <https://doi.org/10.1109/ISIT.2011.6033942>

7 [24] RANGAN, S., SCHNITER, P. and FLETCHER, A. (2014). On the convergence of approximate message
8 passing with arbitrary matrices. In *2014 IEEE International Symposium on Information Theory* 236–
9 240. <https://doi.org/10.1109/ISIT.2014.6874830>

10 [25] RANGAN, S., SCHNITER, P. and FLETCHER, A. K. (2017). Vector approximate message passing. *2017 IEEE
11 International Symposium on Information Theory (ISIT)* 1588–1592.

12 [26] RASKUTTI, G., WAINWRIGHT, M. J. and YU, B. (2011). Minimax Rates of Estimation for High-
13 Dimensional Linear Regression Over ℓ_q -Balls. *IEEE Transactions on Information Theory* **57** 6976–
6994. <https://doi.org/10.1109/TIT.2011.2165799>

14 [27] SCHNITER, P., RANGAN, S. and FLETCHER, A. K. (2016). Vector approximate message passing for the
15 generalized linear model. In *2016 50th Asilomar Conference on Signals, Systems and Computers* 1525–
16 1529. <https://doi.org/10.1109/ACSSC.2016.7869633>

17 [28] TIBSHIRANI, R. (1996). Regression shrinkage and selection via the lasso. *Journal of the Royal Statistical
18 Society, Series B* **58** 267–288.

19 [29] VERZELEN, N. (2012). Minimax risks for sparse regressions: Ultra-high dimensional phenomenons. *Electron. J. Statist.* **6** 38–90. <https://doi.org/10.1214/12-EJS666>

20 [30] VILA, J., SCHNITER, P., RANGAN, S., KRZAKALA, F. and ZDEBOROVÁ, L. (2015). Adaptive damping and
21 mean removal for the generalized approximate message passing algorithm. In *2015 IEEE International
22 Conference on Acoustics, Speech and Signal Processing (ICASSP)* 2021–2025. <https://doi.org/10.1109/ICASSP.2015.7178325>

23 [31] WANG, L. (2013). The L_1 penalized LAD estimator for high dimensional linear regression. *J. Multivariate
24 Anal.* **120** 135–151. 3072722 <https://doi.org/10.1016/j.jmva.2013.04.001>

25 [32] ZHANG, C.-H. (2012). Minimax ℓ_q risk in ℓ_p balls. In *Contemporary Developments in Bayesian Analy-
26 sis and Statistical Decision Theory: A Festschrift for William E. Strawderman* (D. FOURDRINIER,
27 É. MARCHAND and A. L. RUKHIN, eds.). *Collections* **8** 78–89. Institute of Mathematical Statistics,
28 Beachwood, Ohio, USA. <https://doi.org/10.1214/11-IMSCOLL806>

29 [33] ZHENG, L., MALEKI, A., WENG, H., WANG, X. and LONG, T. (2017). Does ℓ_p -Minimization Outperform
30 ℓ_1 -Minimization? *IEEE Transactions on Information Theory* **63** 6896–6935. <https://doi.org/10.1109/TIT.2017.2717585>

31
32
33
34
35
36
37
38
39
40
41
42
43
44
45
46
47
48
49
50
51

1 <author>
2 <author>
3 <author>
4 <author>
5 <author>
6 <author>
7
8 <author>
9 <author>
10 <author>
11
12
13 <author>
14
15 <author>
16
17 <author>
18
19 <author>
20
21
22 <author>
23
24 <author>
25
26
27 <author>
28
29
30 <author>
31
32
33
34
35
36
37
38
39
40
41
42
43
44
45
46
47
48
49
50
51

| | | |
|----|--|----|
| 1 | META DATA IN THE PDF FILE | 1 |
| 2 | Following information will be included as pdf file Document Properties: | 2 |
| 3 | | 3 |
| 4 | Title : Asymptotic risk and phase transition of 11-penalized robust esti- mator | 4 |
| 5 | Author : Hanwen Huang | 5 |
| 6 | Subject : The Annals of Statistics, 0, Vol. 0, No. 00, 1-22 | 6 |
| 7 | Keywords : 62J05, 62J07, 62H12, Mean square error, minimax, penalized, phase transition, robust | 7 |
| 8 | | 8 |
| 9 | | 9 |
| 10 | THE LIST OF URI ADDRESSES | 10 |
| 11 | | 11 |
| 12 | | 12 |
| 13 | Listed below are all uri addresses found in your paper. The non-active uri addresses, if any, are indicated as ERROR. Please check and update the list where necessary. The e-mail addresses are not checked – they are listed just for your information. More information can be found in the support page: http://www.e-publications.org/ims/support/urihelp.html. | 13 |
| 14 | | 14 |
| 15 | | 15 |
| 16 | | 16 |
| 17 | 301 http://www.imstat.org/aos/ [2:pp.1,1] Moved Permanently | 17 |
| 18 | 301 http://www.imstat.org [2:pp.1,1] Moved Permanently // http://www.imstat.org | 18 |
| 19 | --- mailto: huanghw@uga.edu [2:pp.1,1] Check skip | 19 |
| 20 | 301 http://www.ams.org/mathscinet/msc/msc2010.html [2:pp.1,1] Moved Permanently | 20 |
| 21 | 404 https://doi.org/10.1214/19-AOS1923SUPP [4:pp.21,21,22,22] Not Found | 21 |
| 22 | | 22 |
| 23 | | 23 |
| 24 | | 24 |
| 25 | | 25 |
| 26 | | 26 |
| 27 | | 27 |
| 28 | | 28 |
| 29 | | 29 |
| 30 | | 30 |
| 31 | | 31 |
| 32 | | 32 |
| 33 | | 33 |
| 34 | | 34 |
| 35 | | 35 |
| 36 | | 36 |
| 37 | | 37 |
| 38 | | 38 |
| 39 | | 39 |
| 40 | | 40 |
| 41 | | 41 |
| 42 | | 42 |
| 43 | | 43 |
| 44 | | 44 |
| 45 | | 45 |
| 46 | | 46 |
| 47 | | 47 |
| 48 | | 48 |
| 49 | | 49 |
| 50 | | 50 |
| 51 | | 51 |